TNFα-induced LDL cholesterol accumulation involve elevated LDLR cell surface levels and SR-B1 downregulation in human arterial endothelial cells

Emmanuel Ugochukwu Okoro

Department of Microbiology, Immunology, and Physiology, Meharry Medical College, Nashville, TN 37208

Correspondence: Emmanuel U. Okoro
E-mail: eokoro@mmc.edu

Running title: TNFα on arterial endothelial LDL uptake

Keywords: cell surface receptor, cholesterol, endothelial cell, lipoprotein, low-density lipoprotein (LDL), tumor necrosis factor (TNF)

ABSTRACT

Excess lipid droplets are frequently observed in arterial endothelial cells at sites of advanced atherosclerotic plaques. Here, the role of tumor necrosis factor alpha (TNFα) in modulating low density lipoprotein (LDL) content in confluent primary human aortic endothelial cells (pHAECs) was investigated. TNFα promoted up to 2 folds increase in cellular cholesterol, which was resistant to ACAT inhibition. The cholesterol increase was associated with increased ^{125}I-LDL surface binding. Using the non-hydrolysable label, Dil, TNFα could induce a massive increase in Dil-LDL by over 200 folds. The elevated intracellular Dil-LDL was blocked with excess unlabeled LDL and PCSK9, but not oxidized LDL (oxLDL), RAP, or apoE depletion. Moreover, TNFα-induced increase of LDL-derived lipids was elevated through lysosome inhibition. Using specific LDLR antibody, the Dil-LDL accumulation was reduced by over 99%. Effects of TNFα included LDLR cell surface increase by 138%, and very large increases in ICAM-1 total and surface proteins, respectively. In contrast, that of scavenger receptor B1 (SR-B1) was reduced. Additionally, LDLR antibody bound rapidly in TNFα-treated cells by about 30 folds, inducing a migrating shift in the LDLR protein. The effect of TNFα on Dil-LDL accumulation was inhibited by the antioxidant tetramethythiourea (TMTU) dose-dependently, but not by downstream cascade inhibitors against NF-κB, stress kinases, ASK1, JNK, p38, or apoptosis caspases. Grown on transwell inserts, TNFα did not enhance apical (AP) to basolateral (BL) LDL cholesterol or Dil release. It is concluded that TNFα promotes LDLR functions through combined increase at the cell surface and SR-B1 downregulation.

INTRODUCTION

TNFα was originally discovered as a tumor-selective hemorrhagic factor (1,2). However, it is now recognized to have multiple cell-type dependent effects (3,4). Released as a 17 kD soluble protein from a transmembrane precursor by tumor necrosis factor converting enzyme (TACE) (5-7), this cytokine mainly promotes changes that facilitate leukocyte (inflammatory) functions. (3,8). Acting through the rapid-acting transcription factor, nuclear factor kappa B (NF-κB), it can induce expression of pro-inflammatory mediators such as interleukin 1 and 2 (9,10). Likewise, it is capable of inducing apoptosis (11-13), possibly through c-jun N-terminal kinase (JNK) activation (14-16). Thus TNFα may clear way for passage of leukocytes

through target epithelial cell apoptosis. On the other hand, it can induce proliferation of lymphocytes and fibroblasts (12,17-19). This ability to induce proliferation have been reported to be due to upregulation of growth factor receptors (20,21) or growth factor release, such as vascular endothelial growth factor (VEGF) (21-23) .

Background inflammation is an independent risk factor for atherosclerotic cardiovascular disease (24). Serum concentration of TNFα increases with severity of atherosclerotic lesion (25). Thus, it has been reported to be about 200 folds higher in the atherosclerotic lesion than in the circulating blood (26). Further, age (27), infection (28,29), and psycho-environmental stress (30) are associated with elevated TNFα.

The effect of TNFα on atherosclerosis development is mixed. On one hand, it has been reported to promote advanced lesion development (31-34), while suppressing early fatty streak (34). In contrast, antibodies against TNFα have been reported to induce advanced lesions (35). The pro-atherogenic arm of TNFα is in part due to its ability to enhance monocyte entry into the intima through induction of adhesion molecules on arterial endothelial cells. In atherosclerotic lesions, macrophages (36) and smooth muscle cells (36,37) have been found to express TNFα, where it acts on overlying endothelial cells to stimulate expression of leukocyte adhesion molecules such as E-selectin, vascular cell adhesion molecule-1 (VCAM-1), and intercellular adhesion molecule-1 (ICAM-1) (38). More, it induces expression of monocyte chemoattractant protein I (MCP-1) (39), which stimulates gradient migration of lymphocytes and monocytes (40,41).

Beyond its effects on leukocyte-to-endothelial adhesion proteins, the precise mechanism(s) by which TNFα affects atherosclerosis development is poorly understood. For example, tumor necrosis factor receptor 1 (TNFR1) has been reported to be anti-atherogenic (42,43), pro-atherogenic (31,44,45), or neutral (46). Likewise, TNFR2 has been reported to be pro-atherogenic (47) or neutral (43). These conflicting results suggest that the mechanisms by which TNFα affects atherosclerosis development need further clarification, especially at the level of the intima.

Unlike macrophages (48,49) and smooth muscle cells (48,50), normal confluent endothelial cells are resistant to cholesterol accumulation (51). However, fibro-fatty atherosclerotic lesions contain endothelial foam cells with intact monolayer (52-54). In this report, I have studied the effect of TNFα on the pro-atherogenic lipoprotein, LDL (55,56). Importantly, it has been suggested that the pro-atherogenic function of TNFα is related to it effects on non-inflammatory cells of the arterial wall (44). Here, I present evidence of native LDL uptake alteration in pHAECs, which may contribute to the atherogenic nature of TNFα and LDL. It will be shown that TNFα increases pHAEC cholesterol and lipid accumulation by enhancing LDL receptor (LDLR) functions.

RESULTS

TNFα enhances cholesterol accumulation and LDL binding to pHAECs. Atherosclerotic lesion is characterized by release of inflammatory cytokines, among which is TNFα. To evaluate the effect of TNFα on pHAECs cholesterol content, confluent pHAECs were treated with or without TNFα and the cellular cholesterol content was measured. As is shown in **Figure 1A,** TNFα significantly increased unesterified cholesterol, and to a greater degree, esterified cholesterol (**Figure 1B**). To evaluate whether TNFα affects the ability of LDL to bind to the cells, ^{125}I-LDL binding was performed. **Figure 1C** shows that TNFα enhanced ^{125}I-LDL surface releasable ^{125}I-LDL at 4 °C, after the cells were pre-treated at 37 °C. The amount released increased in the presence of 20 folds unlabeled LDL. This indicates that the ^{125}I-LDL bound to some native LDL receptor. Further,

cell-associated ^{125}I-LDL was also higher on TNFα-treated pHAECs (**Figure 1D**).

ACAT inhibitor does not prevent TNFα-induced LDL cholesterol accumulation. It has been reported that TNFα induces cholesteryl ester accumulation in monocytes through enhanced ACAT activity in the presence of oxLDL (57). To evaluate the extent to which enhanced ACAT activity is responsible in raising pHAEC cholesterol in the presence of LDL, the cells were treated with or without ACAT inhibitor, Sandoz 58-035. As is reported in **Figure 2A-B**, inhibition of ACAT activity slightly raised the unesterified cholesterol, and significantly suppressed cholesteryl ester accumulation. Despite this inhibition, the TNFα-induced total cholesterol accumulation, now mainly in the unesterified form, was not prevented (**Figure 2A,C**). ACAT inhibition also reduced the total cholesterol in the cells, with or without TNFα stimulation (**Figure 2C**). This is a known effect of ACAT inhibition. The higher elevated unesterified cholesterol is more likely to be effluxed from the cells than the esterified one (58).

LDL oxidation is not required for TNFα-induced LDL accumulation. Having demonstrated that TNFα promoted LDL binding to pHAECs (Figure 1), the requirement for oxidative modification of LDL was investigated. Particularly, TNFα has been reported to promote release of the reactive oxygen species, superoxide and hydrogen peroxide (59,60). Hence, experiments were performed to determine whether oxidative modification of LDL is a prerequisite to TNFα-induced LDL binding. To visualize TNFα-induced LDL binding and subsequent internalization, Dil-LDL was used. Internalized Dil-LDL was significantly increased through TNFα pre-treatment (**Figure 3A-B**). It can also be seen in **Figure 3A-B** that excess unlabeled native LDL blocked binding and internalization of Dil-LDL, with and without TNFα treatment. This demonstrates that native LDL components, and therefore receptors, are required for Dil-LDL binding and internalization. Excess unlabeled oxLDL, on the other hand, did not prevent Dil-LDL intracellular accumulation in control and TNFα-treated cells. Instead, there was a tendency of oxLDL to enhance intracellular Dil-LDL with or without TNFα.

TNFα induces massive Dil over [^{3}H]CE lipid accumulation from LDL. The lipids, Dil and ^{3}H-cholesteryl esters ([^{3}H]CE), are stably fixed within LDL. To evaluate the ability of pHAECs to retain LDL hydrolysable [^{3}H]CE or the non-hydrolysable Dil, the cells were treated with increasing concentration of TNFα in the presence of [^{3}H]CE-LDL or Dil-LDL. As is shown in **Figure 4A**, ^{3}H-cholesterol accumulation derived from [^{3}H]CE-LDL was increased by about 2 folds with increasing TNFα concentration. On the other hand, Dil accumulation increased by about 50 folds (**Figure 4B**). Next, cells were treated with increasing Dil-LDL concentration without (**Figure 4C**) or with TNFα (**Figure 4D**). As is shown in **Figure 4C**, 400 µg/ml Dil-LDL increased intracellular Dil level by about 50 folds compared to that at 1 µg/ml under control condition. Compared to Ctrl at 400 µg/ml Dil-LDL, TNFα increased the intracellular Dil by over 200 folds (**Figure 4D**).

Lysosomal inhibitor enhances TNFα-induced LDL lipid accumulation. The lowering of pH facilitates disintegration and degradation of internalized LDL by low pH-dependent lysosomal enzymes. This degradation is suppressed by the pH-raising compound, chloroquine (61). To evaluate whether a similar phenomenon occurs in pHAECs, the cells were treated in the presence or absence of chloroquine. The presence of chloroquine caused the Dil to accumulate circumferentially within the cells, presumably in defective lysosomes (**Figure 5A**). As can be seen in **Figure 5A-B**, chloroquine greatly enhanced Dil-LDL accumulation without TNFα. The presence of TNFα further increased the amount of

chloroquine-induced cellular Dil-LDL. Chloroquine also increased ^{3}H-cholesterol level from [^{3}H]CE-LDL. However, it was not as pronounced as in the case of Dil (**Figure 5C**).

ApoE is not required for TNFα-induced Dil-LDL accumulation. Apolipoprotein B (apoB) is the major protein in LDL (62). However, variable amounts of apoE are also present in LDL (63). Since apoE plays a major role in binding several lipoprotein receptors of the LDLR family (64,65), the effect of apoE depletion on TNFα-induced Dil-LDL intracellular levels was investigated. The successful depletion of apoE from Dil-HDL3 and Dil-LDL can be seen in **Figure 6A**. That both HDL3 and LDL contain apoE, while apoA1 and apoB are present in significant amounts only in HDL3 and LDL, respectively, is apparent in the figure. In **Figure 6B**, it can be seen that the isolation procedure did not inhibit the ability of TNFα to induce Dil-LDL accumulation. Further, apoE depletion had no effect in this regard.

TNFα-induced Dil-LDL accumulation is blocked by specific LDLR antibody. Having found evidence that TNFα promotes cholesterol accumulation in pHAECs through enhanced endocytosis of native LDL, I next investigated what members of the LDLR family are responsible. As can be seen in **Figure 7A**, the pan-LDLR family blocker PCSK9 (66-68), but not RAP (69), suppressed the Dil-LDL accumulation. The LDLR family members are abundantly expressed in hepatocytes. Thus, to evaluate whether RAP activity is measurable in hepatocytes, the cells were treated RAP (**Figure 7B**). The results show that the failure of RAP to inhibit Dil-LDL internalization is specific to pHAECs. Since RAP has been reported to be ineffective against LDLR (70), the data point to LDLR as the most likely candidate.

To investigate the contribution of LDLR in mediating TNFα-induced Dil-LDL accumulation, an LDLR antibody was investigated for its specificity and function in pHAECs treated with or without TNFα. As can be seen in **Figure 7C**, the antibody recognized a single protein consistent with the expected migration position of LDLR. It can be seen that incubation of TNFα-treated cells with the antibody induced an upward migratory shift in LDLR protein to a larger extent than in control cells. Attempts to directly detect the LDLR antibody were unsuccessful, suggesting that the shift is due to another interaction or modification.

HDL3 critically depends on non-LDLR mechanisms for uptake, especially in the absence of apoE (71). Thus, to further evaluate the specificity of the LDLR antibody, intracellular uptake of Dil-HDL3 was measured. As can be seen in **Figure 7D**, intracellular Dil-HDL3 levels was significantly blocked by excess unlabeled HDL3, whereas that of LDL only had a mild effect. Further, the LDLR antibody did not block intracellular Dil-HDL3 to a considerable level. In contrast, the LDLR antibody blocked intracellular Dil-LDL accumulation (**Figure 7E**). This blockage was greater than 99% in TNFα-treated cells.

TNFα upregulates cell surface LDLR protein. Having determined that LDLR is responsible for TNFα-induced LDL accumulation in pHAECs, I next tested whether total and surface LDLR is changed by TNFα. As can be seen **in Figure 8A,D**, TNFα-induced upregulation of the LDLR protein total and surface by about 90% and 138%, respectively. ABCA1 (Figure 8A, B) and ICAM-1 (Figure 8A, C) proteins, both of which have been reported to be induced by TNFα treatment (29,72,73), were found to be significantly increased as well. A low molecular weight form of ABCA1, however, was primarily induced in TNFα-treated cells. In contrast, scavenger receptor B1 (SR-B1) was downregulated by TNFα (Figure 8A, E). Similar findings have been reported on hepatocytes (74). Figure 8A also shows that the intracellular proteins GAPDH were undetectable at the cell surface. Although caveolin-1 has been reported

to be closely associated with the inner plasma membrane (75,76), it was not detected in the cell surface assay. This indicates that outer plasma membrane proteins were selectively labeled.

TNFα promotes rapid association of LDLR with its antibody. To evaluate the consequence of the increase in cell surface LDLR induced by TNFα on the association and entry of LDLR antibody, immunofluorescence studies were performed. As can be seen in **Figure 9A**, TNFα did not enhance association of control antibody with the cells, but significantly induced association with the specific LDLR antibody by 30 minutes at 37 °C. This indicates that TNFα did not promote non-selective endocytic processes. The surface distribution of LDLR (arrows) and the internalization of the surface LDLR (arrow heads) in cells treated with TNFα can be seen in **Figure 9B**.

The total amount of surface LDLR bound by the antibody at 37 °C can be seen to increase with time. At 0, 5, 30, and 120 minutes, there was about 30, 50, 7, and 2 folds, respectively, more surface LDLR antibody in TNFα-treated cells compared to control cells at the corresponding time (**Figure 9C-D**). This demonstrates that LDLR antibody rapidly binds surface LDLR in the case of TNFα-treated cells, plateauing by about 2 hours.

Anti-oxidant suppresses TNFα-induced Dil-LDL accumulation. TNFα signaling cascade involves multiple mediators, among which are the transcription factor, NF-κB, and apoptosis signal-regulating kinase 1 (ASK1), an upstream mediator of JNK and p38 (77), that facilitate apoptosis. To evaluate whether these proteins are upstream in the TNFα-induced Dil-LDL accumulation, experiments were performed in the presence of their respective inhibitors. As can be seen in **Figure 10A**, the inhibitors did not suppress the action of TNFα. In contrast, the anti-oxidant, TMTU, inhibited this effect with increasing doses (**Figure 10B**).

TNFα does not affect AP to BL release of degraded LDL protein. To address the effect of increased LDLR-mediated uptake of LDL on apical to basolateral LDL protein transport, the pHAECs were grown to confluence on transwell inserts, as shown in **Figure 11A**. ^{125}I-LDL detected in the BL medium was either non-intact (**Figure 11B**) or intact (**Figure 11C**). In **Figure 11B**, it is shown that unlabeled LDL competitor reduced the amount of non-intact ^{125}I-LDL, indicating release in a receptor-dependent manner. This was TNFα-independent. In contrast, the unlabeled competitor had no effect on the intact ^{125}I-LDL measured in the BL medium (**Figure 11C**). TNFα tended to enhance BL release of intact ^{125}I-LDL, consistent with enhanced cell-cell permeability. The overall data thus indicate that the LDLR protein cargo is not efficiently trafficked in a polarized manner in pHAECs.

TNFα does not affect AP to BL LDL lipid release. To determine whether LDLR facilitates AP to BL LDL lipid transport, the pHAECs on transwell inserts were incubated with LDL colabeled with Dil and ^{3}H-cholesteryl esters (**Figure 12A-B**). As can be seen in the figures, TNFα dose-dependently increased the accumulation of Dil-LDL on the pHAECs grown on transwell inserts, in the same manner as those grown on plastic dishes. Similar to pHAECs on plastic dishes, the LDLR antibody significantly blocked the TNFα-induced uptake of Dil-LDL by pHAECs grown on transwell inserts by over 99%. The corresponding uptake of ^{3}H-cholesteryl esters is shown in **Figure 12C**. The ^{3}H-cholesteryl ester accumulation induced by TNFα is blocked in the presence of antibody against LDLR. Surprisingly, LDLR blockage had no effect on the amount of measurable ^{3}H-choleseryl ester detectable in the BL medium (**Figure 12D**). This is consistent with the BL Dil-LDL, whose value was independent of TNFα treatment (**Figure 12E**).

DISCUSSION

Native LDL modification due to oxidation (78), aggregation (79), or complex formation with proteoglycans (80-83) is known to promote cholesterol accumulation in macrophages. In contrast, confluent arterial endothelial cells are resistant to cholesterol accumulation induced by any of these lipoproteins. My results demonstrate that this can be altered in the presence of TNFα. Thus, LDL modification is not an absolute requirement for LDL-induced cholesterol or lipid accumulation. The data suggest that pHAECs, like macrophages, may be susceptible to changes related to excess cholesterol loading.

Excess cholesterol in arterial endothelial cells is likely to lead to endothelial dysfunction due, in part, to space and membrane disruption (84). General upregulation of the LDLR receptor function through inhibition of PCSK9 have been reported to benefit against coronary artery disease (85,86). Notwithstanding, PCSK9 also downregulates other receptors in the LDLR family (67,68), and binds the scavenger receptor, CD36, concurrent with thrombosis (85,87). Thus, the effect of increasing LDLR in the athero-protective effects of PCSK9, beyond lowering serum LDL concentration, is more complex. Interestingly, unlike PCSK9, which lowers LDLR protein (68), I found that specific blocking antibody against LDLR did not cause a major change in the LDLR protein (Figure 7). Instead, it induced a shift in the protein, which indicates that LDLR may signal under appropriate circumstances. Of significance, LDLR has been implicated in non-LDL uptake mechanisms. For example, it has been reported to have anti-apoptotic and anti-inflammatory properties (88). Hence, this receptor plays important roles beyond plasma LDL regulation. Indiscriminate suppression may have subtle negative consequences.

The results from this report indicate that pHAECs have efficient mechanism(s) of getting rid of LDL-derived cholesterol. TNFα induced about 25 folds intracellular Dil-LDL compared to [^{3}H]CE-LDL. Thus it appears that pHAECs are normally protected against LDL-derived cholesterol accumulation by keeping cell surface LDLR down, combined with efficient efflux mechanisms. The TNFα-induction of ABCA1 (Figure 8), which mediates cholesterol efflux, suggest that ABCA1 may be involved. However, the significance of an apparently truncated form (Figure 8A) is unclear. The tendency of TNFα to induce ABCA1 expression in some cell types has also been published by others. Specifically, it has been reported that TNFα enhances cholesterol efflux and ABCA1 mRNA and protein through NF-kB signaling (73) in macrophages, and possibly adipocytes (89). However, as is often characteristic of the complex nature of TNFα signaling, it has also been reported to downregulate ABCA1 in hepatocytes (90), Caco-2 intestinal cell(91), and osteocytes (92).

TNFα is a pleiotropic autocrine and paracrine mediator important in multiple signaling cascades that range from activating immune cells to fight viruses, bacteria, and cancer cells, to promoting entry of monocytes and lymphocytes into atherosclerotic lesions (4,93,94). The latter process is recognized to be pro-atherogenic. TNFα has also been reported to play an important role in the current COVID-19 pandemic (95). Thus, nonspecific disruption of TNFα activity in the animal interferes with many important biological functions (96). It has also been reported that TNFα upregulates LDLR in hepatocytes (90). My finding that TNFα upregulates surface LDLR function in pHAECs implies that it is possible to regulate this process selectively, while leaving the beneficial functions of TNFα intact.

It has been reported that AP to BL LDL transport occurs in vivo across arterial endothelial cells (97). My findings suggest that this transport is probably not through LDLR, as lysosome inhibition (Figure 5) significantly promoted Dil-LDL accumulation with or

without TNFα. SR-BI, on the other hand, has been reported to faciliate AP to BL transport of LDL in an LDLR-independent manner (98). However, there is some controversy about the role of LDLR in trafficking ligand across the brain endothelium. Thus, it has been reported that LDLR mediates transcytosis of LDL and its ligand in brain microvascular endothelial cells (99) in vitro. However, studies using animal models suggest that LRP and very low density lipoprotein receptor (VLDLR), not LDLR, are responsible for the transcytosis (100). Likewise, the binding of LDLR to RAP is controversial. On one hand, it has been reported to bind LDLR (101), while others report the opposite (70). My data suggest that if it binds LDLR, it does not interfere with the ability of LDLR to subsequently internalize LDL.

In summary, the action of TNFα on LDL uptake in pHAECs is due to cell surface upregulation of LDLR, combined with downregulation of SR-B1. Because SR-B1 is also a receptor for LDL, its downregulation promotes preferential binding and internalization through LDLR. Unlike SR-B1 which does not promote net LDL cholesterol accumulation in cells (100), LDLR is a potent inducer of LDL-derived cholesterol storage due to trafficking of its cargo to lysosomes.

EXPERIMENTAL PROCEDURES

Cell culture and incubations. pHAECs (passages 3-7) were maintained in VBM with growth factor kit (VEGF) in the presence of 15% FBS, and antibiotic, antimycotic (100 units/mL of penicillin, 100 µg/mL of streptomycin, and 0.25 µg/mL of amphotericin B. Under serum-free conditions, the cells were cultured in VBM, VEGF, with the latter antimicrobials and 0.1% FAF-BSA. Incubations were at 37 °C, unless indicated otherwise. Experiments were best started with pHAECs confluent for 5 days or longer. Separate cells from individuals (2-36 years old) were used during the course of the experiments, with similar results. Incubations were 24 ± 5 hours. For cell-associated studies at 37 ºC, cells were washed 3X with mHBSS at 0 ºC. Imaging studies demonstrated that the vast majority of Dil-lipoproteins were within the cell under these conditions. For intracellular LDL levels, pHAECs were incubated at 0 °C for 5 minutes with ice cold 400 units/ml sodium heparin in mHBSS, washed twice with the same buffer, then two more times with ice cold mHBSS, to remove surface LDL. In experiments using excess unlabeled lipoproteins, the volume represented 3% or less of the culture medium. Lipids were extracted as described below or the cells were fixed with 4% paraformaldehyde in PBS prior to microscopy.

Materials.

Reagents	Company	Catalog number
[^{3}H]Cholesterol	Perkin Elmer	NET139001
ABCA1 antibody	Santa Cruz Biotechnology	sc-58219
Antibiotic-antimycotic	Thermo Fisher Scientific	15240112
Anti-goat-HRP	R&D Systems	NL001
ApoE antibody	Santa Cruz Biotechnology	sc-13521
ApoE-conjugated agarose	Santa Cruz Biotechnology	sc-13521 AC
ASK 1 inhibitor	Tocris	MSC 2032964A
BCA assay kit	Thermo Fisher Scientific	23227
Bond elut column	Agilent Technologies	12256060
Caspase inhibitor	Tocris	2163
Caveolin-1 antibody	Santa Cruz Biotechnology	sc-53564
Centrifugal filter	Pall Corporation	MAP003C36
Cholesterol esterase	MP Biomedicals	105439
Cholesterol oxidase	Sigma-Aldrich	C8649
Desalting columns	Thermo Fisher Scientific	89890
Dialysis membrane	Spectrum Labs	131204
Dil	Sigma-Aldrich	468495
EZ-link-Biotin	Thermo Fisher Scientific	A39258
FAF-BSA	Sigma-Aldrich	A8806
FBS	R&D Systems	S11550
Glass bottom dishes	Cellvis	P96-0-N
HRP	Alfa Aesar	J60026
ICAM1 antibody	Santa Cruz Biotechnology	sc-107
Iodination beads	Thermo Fisher Scientific	28665
JNK inhibitor	Sigma-Aldrich	420118
LDLR antibody	R&D Systems	AF2148
mHBSS	Sigma-Aldrich	H8264
NF-kB Inhibitor	Sigma-Aldrich	481412
NF-kB Inhibitor	Tocris	4590
Normal goat IgG	R&D Systems	AB-108-C
Normal mouse Ig agarose	Santa Cruz Biotechnology	sc-2343
p38 inhibitor	Sigma-Aldrich	506163
PCSK9	Caymen Chemical	20631
pHAECs	ATCC	PCS-100-011
Phosphatase inhibitor	Sigma-Aldrich	P0044
Protease inhibitor	Sigma-Aldrich	P8340
RAP	Enzo Life Sciences	BML-SE552-0100
Sandoz 58-035	Sigma-Aldrich	S9318
Scopoletin	TCI America	S0367
Sodium heparin	Thermo Fisher Scientific	J16920-EXT
Sodium taurocholate	Beantown Chemicals	141920
SR-B1	Novus Biologicals	NB400-104
Strepavidin mag seph	GE Healthcare	28-9872-30
TMTU	Alfa Aesar	L13392
TNFα	ProSci Inc	96-734
VBM	ATCC	PCS-100-030
VEGF	ATCC	PCS-100-041

Lipoprotein purification. All procedures were performed between 0 and 4 °C. Centrifugations and dialysis were performed at 4 °C. Lipoproteins were isolated from freshly drawn human blood anticoagulated with Na_2EDTA. The blood was centrifuged at 4,000 g for 30 minutes to obtain the plasma. To the plasma, butylated hydroxytoluene (BHT) in DMSO was added to 45 µM (0.01%). Then, sequential density ultracentrifugations (102) were performed to obtain d<1.006 (VLDL), d=1.019-1.063 (LDL), or d=1.12-1.21 (HDL3) g/ml. Ultracentrifugations were done using type Ti70 rotor at 50,000 rpm for 20 (VLDL and LDL) or 48 hours (HDL3). The lipoproteins were dialyzed through ~4 kD molecular weight cut-off membrane in 3 successions against ~180 times dialysis buffer (DB): 10 mM Tris-HCl, 150 mM NaCl, 0.3 mM Na_2EDTA, pH 7.5, with deionized water, in the dark, each lasting about 24 hours. After concentration using 3 kD MWCO centrifugal filters, the LDL was filtered through 0.2 µm membrane under sterile conditions. Lipoprotein contents were routinely verified by western blotting and coomassie staining. In addition, the cholesterol and cholesteryl ester contents were verified to be consistent with previous publications (103-105). Lipoprotein concentrations represent the protein content throughout the manuscript.

Cellular cholesterol determination. Lipids were extracted into hexane: isopropanol (1:1) at room temperature for 3 hours, then the solvent was evaporated at room temperature using centrivap concentrator (Labconco). The extracted lipids were redissolved in isopropanol. To determine the unesterified cholesterol content, the lipids in isopropanol were mixed with 10 times volumes of cholesterol assay buffer (CAB): 0.1% FAF-BSA, 2 mM sodium taurocholate, 50 mM Tris-HCl, pH 7.5, 0.3 mM Na_2EDTA, 5% isopropanol, and 250 mM sucrose, with freshly added 0.5 U/ml horseradish peroxidase (HRP) and 0.02 U/ml cholesterol oxidase in the presence of 30-50 µM scopoletin (106) (excitation 360, emission 460). The CAB was kept at room temperature to ensure full solubilization of the lipids. This enzymatic approach is a modification of a previously published procedure (107). Total cholesterol was determined as above, with the addition of 0.1 U/ml cholesteryl esterase. Readings were obtained after incubation at 37 °C for 20 minutes. Cholesteryl esters were determined by subtracting unesterified cholesterol from the total cholesterol. The residual cell matter after lipid extraction was lysed with 0.1 M NaOH, 0.1% SDS, for protein reading using BCA assay kit.

^{3}H-cholesteryl ester ([^{3}H]CE) generation. 40 µCi of ^{3}H-cholesterol in ethanol was added in 10 µl aliquots to 40 ml of 0.2 µm filtered human serum under sterile conditions. The mixture was incubated at 37 °C for 48 hours in the dark. ^{3}H-cholesteryl esters and other lipids were extracted into chloroform: methanol (108). After evaporation of the solvent, the residue was dissolved in a minimal volume of chloroform. Subsequently, ^{3}H-cholesteryl esters were purified using serial bond elut columns with several hexane passages, as previously described (109).

Western blotting. pHAECs were lysed with lysis buffer (150 mM NaCl, 2% Triton X-100, 20 mM HEPES, pH 7.4, 2% protease inhibitor and 2% phosphatase inhibitor by sonication at 2 setting (Fisher sonic dismembrator model 100) on ice for 10 seconds. After centrifugation at 16,000 g x 10 minutes at 4 °C, equal volume of loading buffer (8 M urea, 2% SDS, 125 mM Tris-HCl, pH 7.0, 5% glycerol, 10% beta-mercaptoethanol, 0.06% bromphenol blue) was mixed with the supernatant at room temperature. This was followed by electrophoresis, electrical transfer to PVDF membrane, and immunoblotting.

Dil- and/or [^{3}H]CE-Lipoproteins. Generation of Dil-labeled lipoproteins was obtained

essentially as previously described (110), with minor modifications. In brief, a mixture of about 2 mg HDL3, LDL, or VLDL protein and 7 ml of human lipoprotein deficient serum was mixed with ~1 mg [^{3}H]CE and/or 0.5 mg Dil in 10 µl DMSO aliquots under sterile conditions. After covering with foil, the mixture was incubated at 37 °C for 21 hours. The lipoproteins were repurified as described above, after adjusting to their respective densities with solid KBr. Combined Dil, [^{3}H]CE-LDL radioactivity was 8.1 dpm/µg protein.

LDL iodination with Na^{125}I. About 2 mg LDL protein in PBS and 10 iodination beads were incubated with Na^{125}I for 10 minutes at room temperature in glass vials. The transformation was stopped with 50 mM each of unlabeled sodium iodide and sulfite, and 100 µM BHT in DMSO (0.01%). The labeled LDL was washed with desalting columns, then passed through centrifugal filters, 3 kD MWCO, against dialysis buffer.

^{125}I-LDL cell surface binding. Confluent pHAECs on plastic dishes were cultured with 0 or 5 ng/ml TNFα in 15% serum for 48 hours. Treatment continued with serum-free medium in the continued presence of TNFα for 3 hours to deplete surface-bound LDL. Subsequently, ^{125}I-LDL was added to 15 µg/ml for 1 hour at 37 °C. The cells were then washed two times with PBS at room temperature, then chilled on ice. Afterwards, serum-free medium at 4 °C with 0 (buffer) or 300 µg/ml LDL was added. Following additional incubation at 4 °C for 1 hour, the radioactivity released to the medium was taken as surface-releasable ^{125}I-LDL.

LDL oxidation. LDL was dialysed against PBS at 4 °C, passed through 0.2 µm filter, and incubated at 37 °C for 22 hours with 5 µM $CuSO_4$ in PBS under sterile conditions. After adding BHT in DMSO (0.005%) to 1 µM and Na_2EDTA to 10 mM, the mixture was dialysed against dialysis buffer, and finally filtered through 0.2 µm membrane under sterile conditions.

TBARS Assay. 2-thiobarbituric assay to estimate the extent of LDL oxidation was determined essentially as previously described (111), with some modifications. oxLDL was mixed successively with 3 volumes of 0.67% 2-thiobarbituric acid in 50 mM NaOH and 20% trichloroacetic acid, each containing 1 mM Na_2EDTA, respectively. After heating at 55 °C for 1 hour, the mixture was centrifuged at 16,000 g x 30 seconds. Fluorescence (530 nm excitation, 590 nm emission) reading in the supernatant was determined. Malonaldehyde bis-(dimethyl acetal) was used as a malondialdehyde (MDA) precursor for determining malondialdehyde standards. Care should be taken when performing this procedure, as volatile products are generated at 100 °C. Standards up to 5 nmol/ul were used. oxLDL was measured at 54 nmol MDA equivalents/ mg protein.

Depletion of apoE from Dil-lipoproteins. Normal mouse IgG agarose or apoE3 agarose beads were washed 4X with dialysis buffer under sterile conditions. Subsequently, Dil-HDL3 or Dil-LDL was added to the beads in dialysis buffer. Following 24 hour incubation at 4 °C, the unbound lipoproteins were sterile filtered through 0.2 µm membranes.

Cell surface biotinylation. Serum media from confluent pHAECs were replaced with 400 U/ml sodium heparin in mHBSS on ice for 5 minutes, washed 2X with the the same buffer, then 1X with ice cold mHBSS. After 1X wash with ice cold 1X PBS, the cells were treated with EZ Link Sulfo NHS Biotin in 1X PBS for 30 minutes at 4 °C. Unreacted biotin reagent was quenched with 100 mM glycine in PBS at 4 °C for 5 minutes. Following 1X wash with ice cold mHBSS, the cells were lysed on the plates with lysis buffer as indicated above under Western blotting on ice for 30 minutes, followed by sonication at 2 setting for 10 seconds on ice.

Aliquots of the supernatant was mixed with 1 volume of 2X urea loading buffer without heating. The rest of the supernatant was mixed with strepavidin mag sepharose (pre-washed 2X with incubation buffer: 1% BSA, 0.1% NaN3, 0.1% Triton X-100). After 10X dilution with the incubation buffer containing 0.5% each of protease inhibitor and phosphate inhibitor cocktails, the suspension was swirled for 12 hrs at 4 °C. The beads were washed 4X with precipitation buffer, then mHBSS at 4 °C. After 1X urea loading buffer (1:1 volume of lysis buffer and 2X urea loading buffer), with 1% protease and phosphatase inhibitors, respectively, the samples were heated at 95 °C for 5 minutes to solubilize the bound biotinylated proteins.

Dextran-Mn separation of intact and non-intact ^{125}I-LDL. Intact ^{125}I-LDL was separated from non-intact LDL using dextran sulfate, Mn^{2+} procedure essentially as previously described (112). To the BL medium, d<1.21 g/ml FBS was added to 15% to produce a visible precipitate, mixed, then dextran sulfate and MnCl were added to 65 mg/ml and 0.2 M, respectively. After incubation for 20 minutes at room temperature, the mixtures were centrifuged at 5000 g x 5 minutes at 4 °C. The pellet was redissolved with 20 mg/ml dextran sulfate before scintillation counting.

Immunofluorescence. Confluent pHAECs in serum medium were incubated with 0 or 100 ng/ml TNFα for 24 hours. Subsequently, the media were replaced with serum-free medium containing 10 µg/ml normal goat IgG or LDLR Ab (R&D Systems) in the continued presence of 0 or 100 ng/ml TNFα for 0, 5, 30, or 120 minutes at 37 ºC. Afterwards, the cells were chilled on ice and further incubated at 4 ºC for 1 hour. Then the cells were washed 2X with ice-cold mHBSS, fixed with ice-cold methanol at -20 ºC for 10 minutes, washed once with mHBSS at room temperature, then blocked with 50% human serum in mHBSS, 0.1% sodium azide (blocking buffer) for 1 hour at room temperature. Afterwards, it was replaced with 4 µg/ml red antigoat antibody in blocking buffer. Following 30 minute incubation at room temperature, the medium was replaced with mHBSS, washed 3X with blocking buffer (10 minutes each at room temperature), fixed with 4% paraformaldehyde in PBS, followed by fluorescence microscopy.

Fluorescence Microscopy. Fluorescence microscopy was performed using Keyence phase-contrast fluorescence microscope. Images were analyzed using CellProfiler (113). Confocal microscopy was performed using glass bottom dishes (Cellvis).

STATISTICAL ANALYSIS. Data are reported as averages ± standard deviation. n = number of independent experiments performed on separate days. Most experiments were performed with an average of 3 or greater replicates. Analysis of variance, followed by Tukey post hoc testing was done by using statpages.info website.

DATA AVAILABILITY. All data are contained in the manuscript.

ACKNOWLEDGMENTS. The author thanks the Meharry core facility staff for assistance in the using the equipment.

FUNDING
This work was supported through the following grants: Meharry Clinical and Translation Research Center (MeTRC) 5U54MD007593-09 (EUO, Samuel Adunyah), RCMI 5U54MD007586-33 (EUO, Samuel Adunyah), SC1HL101431(Hong Yang). Confocal microscopy core was supported through NIH grants MHD007586 and S10RR025497. The content is solely the responsibility of the author and does not necessarily represent the official views of the National Institutes of Health.

CONFLICT OF INTEREST
The author declares that he has no conflicts of interest with the contents of this article

REFERENCES

1. Carswell, E. A., Old, L. J., Kassel, R. L., Green, S., Fiore, N., and Williamson, B. (1975) An endotoxin-induced serum factor that causes necrosis of tumors. *Proc. Natl. Acad. Sci. U. S. A.* **72**, 3666-3670
2. Balkwill, F. (2009) Tumour necrosis factor and cancer. *Nat. Rev. Cancer* **9**, 361-371
3. Holbrook, J., Lara-Reyna, S., Jarosz-Griffiths, H., and McDermott, M. (2019) Tumour necrosis factor signalling in health and disease. *F1000Res* **8**
4. Mercogliano, M. F., Bruni, S., Elizalde, P. V., and Schillaci, R. (2020) Tumor Necrosis Factor alpha Blockade: An Opportunity to Tackle Breast Cancer. *Front Oncol* **10**, 584
5. Kriegler, M., Perez, C., DeFay, K., Albert, I., and Lu, S. D. (1988) A novel form of TNF/cachectin is a cell surface cytotoxic transmembrane protein: ramifications for the complex physiology of TNF. *Cell* **53**, 45-53
6. Jue, D. M., Sherry, B., Luedke, C., Manogue, K. R., and Cerami, A. (1990) Processing of newly synthesized cachectin/tumor necrosis factor in endotoxin-stimulated macrophages. *Biochemistry* **29**, 8371-8377
7. Black, R. A., Rauch, C. T., Kozlosky, C. J., Peschon, J. J., Slack, J. L., Wolfson, M. F., Castner, B. J., Stocking, K. L., Reddy, P., Srinivasan, S., Nelson, N., Boiani, N., Schooley, K. A., Gerhart, M., Davis, R., Fitzner, J. N., Johnson, R. S., Paxton, R. J., March, C. J., and Cerretti, D. P. (1997) A metalloproteinase disintegrin that releases tumour-necrosis factor-alpha from cells. *Nature* **385**, 729-733
8. Sedger, L. M., and McDermott, M. F. (2014) TNF and TNF-receptors: From mediators of cell death and inflammation to therapeutic giants - past, present and future. *Cytokine Growth Factor Rev.* **25**, 453-472
9. Hiscott, J., Marois, J., Garoufalis, J., D'Addario, M., Roulston, A., Kwan, I., Pepin, N., Lacoste, J., Nguyen, H., Bensi, G., and et al. (1993) Characterization of a functional NF-kappa B site in the human interleukin 1 beta promoter: evidence for a positive autoregulatory loop. *Mol. Cell. Biol.* **13**, 6231-6240
10. Paliogianni, F., Raptis, A., Ahuja, S. S., Najjar, S. M., and Boumpas, D. T. (1993) Negative transcriptional regulation of human interleukin 2 (IL-2) gene by glucocorticoids through interference with nuclear transcription factors AP-1 and NF-AT. *J. Clin. Invest.* **91**, 1481-1489
11. Laster, S. M., Wood, J. G., and Gooding, L. R. (1988) Tumor necrosis factor can induce both apoptic and necrotic forms of cell lysis. *J. Immunol.* **141**, 2629-2634
12. Sugarman, B. J., Aggarwal, B. B., Hass, P. E., Figari, I. S., Palladino, M. A., Jr., and Shepard, H. M. (1985) Recombinant human tumor necrosis factor-alpha: effects on proliferation of normal and transformed cells in vitro. *Science* **230**, 943-945
13. Frater-Schroder, M., Risau, W., Hallmann, R., Gautschi, P., and Bohlen, P. (1987) Tumor necrosis factor type alpha, a potent inhibitor of endothelial cell growth in vitro, is angiogenic in vivo. *Proc. Natl. Acad. Sci. U. S. A.* **84**, 5277-5281
14. Verheij, M., Bose, R., Lin, X. H., Yao, B., Jarvis, W. D., Grant, S., Birrer, M. J., Szabo, E., Zon, L. I., Kyriakis, J. M., Haimovitz-Friedman, A., Fuks, Z., and Kolesnick, R. N. (1996) Requirement for ceramide-initiated SAPK/JNK signalling in stress-induced apoptosis. *Nature* **380**, 75-79
15. Sluss, H. K., Barrett, T., Derijard, B., and Davis, R. J. (1994) Signal transduction by tumor necrosis factor mediated by JNK protein kinases. *Mol. Cell. Biol.* **14**, 8376-8384
16. Aoki, H., Kang, P. M., Hampe, J., Yoshimura, K., Noma, T., Matsuzaki, M., and Izumo, S. (2002) Direct activation of mitochondrial apoptosis machinery by c-Jun N-terminal kinase in adult cardiac myocytes. *J. Biol. Chem.* **277**, 10244-10250

17. Scheurich, P., Thoma, B., Ucer, U., and Pfizenmaier, K. (1987) Immunoregulatory activity of recombinant human tumor necrosis factor (TNF)-alpha: induction of TNF receptors on human T cells and TNF-alpha-mediated enhancement of T cell responses. *J. Immunol.* **138**, 1786-1790
18. Vilcek, J., Palombella, V. J., Henriksen-DeStefano, D., Swenson, C., Feinman, R., Hirai, M., and Tsujimoto, M. (1986) Fibroblast growth enhancing activity of tumor necrosis factor and its relationship to other polypeptide growth factors. *J. Exp. Med.* **163**, 632-643
19. Bruggeman, L. A., Drawz, P. E., Kahoud, N., Lin, K., Barisoni, L., and Nelson, P. J. (2011) TNFR2 interposes the proliferative and NF-kappaB-mediated inflammatory response by podocytes to TNF-alpha. *Lab. Invest.* **91**, 413-425
20. Jelinek, D. F., and Lipsky, P. E. (1987) Enhancement of human B cell proliferation and differentiation by tumor necrosis factor-alpha and interleukin 1. *J. Immunol.* **139**, 2970-2976
21. Ligresti, G., Aplin, A. C., Zorzi, P., Morishita, A., and Nicosia, R. F. (2011) Macrophage-derived tumor necrosis factor-alpha is an early component of the molecular cascade leading to angiogenesis in response to aortic injury. *Arterioscler. Thromb. Vasc. Biol.* **31**, 1151-1159
22. Chu, S. C., Tsai, C. H., Yang, S. F., Huang, F. M., Su, Y. F., Hsieh, Y. S., and Chang, Y. C. (2004) Induction of vascular endothelial growth factor gene expression by proinflammatory cytokines in human pulp and gingival fibroblasts. *J. Endod.* **30**, 704-707
23. Maloney, J. P., and Gao, L. (2015) Proinflammatory Cytokines Increase Vascular Endothelial Growth Factor Expression in Alveolar Epithelial Cells. *Mediators Inflamm.* **2015**, 387842
24. Quispe, R., Michos, E. D., Martin, S. S., Puri, R., Toth, P. P., Al Suwaidi, J., Banach, M., Virani, S. S., Blumenthal, R. S., Jones, S. R., and Elshazly, M. B. (2020) High-Sensitivity C-Reactive Protein Discordance With Atherogenic Lipid Measures and Incidence of Atherosclerotic Cardiovascular Disease in Primary Prevention: The ARIC Study. *J Am Heart Assoc* **9**, e013600
25. Yuan, S., Carter, P., Bruzelius, M., Vithayathil, M., Kar, S., Mason, A. M., Lin, A., Burgess, S., and Larsson, S. C. (2020) Effects of tumour necrosis factor on cardiovascular disease and cancer: A two-sample Mendelian randomization study. *EBioMedicine* **59**, 102956
26. Rus, H. G., Niculescu, F., and Vlaicu, R. (1991) Tumor necrosis factor-alpha in human arterial wall with atherosclerosis. *Atherosclerosis* **89**, 247-254
27. Paolisso, G., Rizzo, M. R., Mazziotti, G., Tagliamonte, M. R., Gambardella, A., Rotondi, M., Carella, C., Giugliano, D., Varricchio, M., and D'Onofrio, F. (1998) Advancing age and insulin resistance: role of plasma tumor necrosis factor-alpha. *Am. J. Physiol.* **275**, E294-299
28. Byl, B., Roucloux, I., Crusiaux, A., Dupont, E., and Deviere, J. (1993) Tumor necrosis factor alpha and interleukin 6 plasma levels in infected cirrhotic patients. *Gastroenterology* **104**, 1492-1497
29. Nagashima, S., Mendes, M. C., Camargo Martins, A. P., Borges, N. H., Godoy, T. M., Miggiolaro, A., da Silva Deziderio, F., Machado-Souza, C., and de Noronha, L. (2020) Endothelial Dysfunction and Thrombosis in Patients With COVID-19-Brief Report. *Arterioscler. Thromb. Vasc. Biol.* **40**, 2404-2407
30. Liu, Y. N., Peng, Y. L., Liu, L., Wu, T. Y., Zhang, Y., Lian, Y. J., Yang, Y. Y., Kelley, K. W., Jiang, C. L., and Wang, Y. X. (2015) TNFalpha mediates stress-induced depression by upregulating indoleamine 2,3-dioxygenase in a mouse model of unpredictable chronic mild stress. *Eur. Cytokine Netw.* **26**, 15-25
31. Branen, L., Hovgaard, L., Nitulescu, M., Bengtsson, E., Nilsson, J., and Jovinge, S. (2004) Inhibition of tumor necrosis factor-alpha reduces atherosclerosis in apolipoprotein E knockout mice. *Arterioscler. Thromb. Vasc. Biol.* **24**, 2137-2142
32. Canault, M., Peiretti, F., Mueller, C., Kopp, F., Morange, P., Rihs, S., Portugal, H., Juhan-Vague, I., and Nalbone, G. (2004) Exclusive expression of transmembrane TNF-alpha in mice reduces the inflammatory response in early lipid lesions of aortic sinus. *Atherosclerosis* **172**, 211-218

33. Ohta, H., Wada, H., Niwa, T., Kirii, H., Iwamoto, N., Fujii, H., Saito, K., Sekikawa, K., and Seishima, M. (2005) Disruption of tumor necrosis factor-alpha gene diminishes the development of atherosclerosis in ApoE-deficient mice. *Atherosclerosis* **180**, 11-17
34. Boesten, L. S., Zadelaar, A. S., van Nieuwkoop, A., Gijbels, M. J., de Winther, M. P., Havekes, L. M., and van Vlijmen, B. J. (2005) Tumor necrosis factor-alpha promotes atherosclerotic lesion progression in APOE*3-Leiden transgenic mice. *Cardiovasc. Res.* **66**, 179-185
35. Oberoi, R., Vlacil, A. K., Schuett, J., Schosser, F., Schuett, H., Tietge, U. J. F., Schieffer, B., and Grote, K. (2018) Anti-tumor necrosis factor-alpha therapy increases plaque burden in a mouse model of experimental atherosclerosis. *Atherosclerosis* **277**, 80-89
36. Barath, P., Fishbein, M. C., Cao, J., Berenson, J., Helfant, R. H., and Forrester, J. S. (1990) Detection and localization of tumor necrosis factor in human atheroma. *Am. J. Cardiol.* **65**, 297-302
37. Barath, P., Fishbein, M. C., Cao, J., Berenson, J., Helfant, R. H., and Forrester, J. S. (1990) Tumor necrosis factor gene expression in human vascular intimal smooth muscle cells detected by in situ hybridization. *Am. J. Pathol.* **137**, 503-509
38. Zhang, X., Bishawi, M., Zhang, G., Prasad, V., Salmon, E., Breithaupt, J. J., Zhang, Q., and Truskey, G. A. (2020) Modeling early stage atherosclerosis in a primary human vascular microphysiological system. *Nat Commun* **11**, 5426
39. Zeiher, A. M., Fisslthaler, B., Schray-Utz, B., and Busse, R. (1995) Nitric oxide modulates the expression of monocyte chemoattractant protein 1 in cultured human endothelial cells. *Circ. Res.* **76**, 980-986
40. Carr, M. W., Roth, S. J., Luther, E., Rose, S. S., and Springer, T. A. (1994) Monocyte chemoattractant protein 1 acts as a T-lymphocyte chemoattractant. *Proc. Natl. Acad. Sci. U. S. A.* **91**, 3652-3656
41. Deshmane, S. L., Kremlev, S., Amini, S., and Sawaya, B. E. (2009) Monocyte chemoattractant protein-1 (MCP-1): an overview. *J. Interferon Cytokine Res.* **29**, 313-326
42. Schreyer, S. A., Peschon, J. J., and LeBoeuf, R. C. (1996) Accelerated atherosclerosis in mice lacking tumor necrosis factor receptor p55. *J. Biol. Chem.* **271**, 26174-26178
43. Schreyer, S. A., Vick, C. M., and LeBoeuf, R. C. (2002) Loss of lymphotoxin-alpha but not tumor necrosis factor-alpha reduces atherosclerosis in mice. *J. Biol. Chem.* **277**, 12364-12368
44. Zhang, L., Peppel, K., Sivashanmugam, P., Orman, E. S., Brian, L., Exum, S. T., and Freedman, N. J. (2007) Expression of tumor necrosis factor receptor-1 in arterial wall cells promotes atherosclerosis. *Arterioscler. Thromb. Vasc. Biol.* **27**, 1087-1094
45. Xanthoulea, S., Thelen, M., Pottgens, C., Gijbels, M. J., Lutgens, E., and de Winther, M. P. (2009) Absence of p55 TNF receptor reduces atherosclerosis, but has no major effect on angiotensin II induced aneurysms in LDL receptor deficient mice. *PLoS One* **4**, e6113
46. Blessing, E., Bea, F., Kuo, C. C., Campbell, L. A., Chesebro, B., and Rosenfeld, M. E. (2004) Lesion progression and plaque composition are not altered in older apoE-/- mice lacking tumor necrosis factor-alpha receptor p55. *Atherosclerosis* **176**, 227-232
47. Chandrasekharan, U. M., Mavrakis, L., Bonfield, T. L., Smith, J. D., and DiCorleto, P. E. (2007) Decreased atherosclerosis in mice deficient in tumor necrosis factor-alpha receptor-II (p75). *Arterioscler. Thromb. Vasc. Biol.* **27**, e16-17
48. Ross, R., Wight, T. N., Strandness, E., and Thiele, B. (1984) Human atherosclerosis. I. Cell constitution and characteristics of advanced lesions of the superficial femoral artery. *Am. J. Pathol.* **114**, 79-93
49. Hoff, H. F., and Morton, R. E. (1985) Lipoproteins containing apo B extracted from human aortas. Structure and function. *Ann. N. Y. Acad. Sci.* **454**, 183-194

50. Mahley, R. W., Innerarity, T. L., Weisgraber, K. H., and Fry, D. L. (1977) Canine hyperlipoproteinemia and atherosclerosis. Accumulation of lipid by aortic medial cells in vivo and in vitro. *Am. J. Pathol.* **87**, 205-226
51. Vlodavsky, I., Fielding, P. E., Fielding, C. J., and Gospodarowicz, D. (1978) Role of contact inhibition in the regulation of receptor-mediated uptake of low density lipoprotein in cultured vascular endothelial cells. *Proc. Natl. Acad. Sci. U. S. A.* **75**, 356-360
52. Poole, J. C., and Florey, H. W. (1958) Changes in the endothelium of the aorta and the behaviour of macrophages in experimental atheroma of rabbits. *J. Pathol. Bacteriol.* **75**, 245-251
53. Simionescu, M. (2007) Implications of early structural-functional changes in the endothelium for vascular disease. *Arterioscler. Thromb. Vasc. Biol.* **27**, 266-274
54. Joris, I., Zand, T., Nunnari, J. J., Krolikowski, F. J., and Majno, G. (1983) Studies on the pathogenesis of atherosclerosis. I. Adhesion and emigration of mononuclear cells in the aorta of hypercholesterolemic rats. *Am. J. Pathol.* **113**, 341-358
55. Zhang, Y., Vittinghoff, E., Pletcher, M. J., Allen, N. B., Zeki Al Hazzouri, A., Yaffe, K., Balte, P. P., Alonso, A., Newman, A. B., Ives, D. G., Rana, J. S., Lloyd-Jones, D., Vasan, R. S., Bibbins-Domingo, K., Gooding, H. C., de Ferranti, S. D., Oelsner, E. C., and Moran, A. E. (2019) Associations of Blood Pressure and Cholesterol Levels During Young Adulthood With Later Cardiovascular Events. *J. Am. Coll. Cardiol.* **74**, 330-341
56. Boren, J., Chapman, M. J., Krauss, R. M., Packard, C. J., Bentzon, J. F., Binder, C. J., Daemen, M. J., Demer, L. L., Hegele, R. A., Nicholls, S. J., Nordestgaard, B. G., Watts, G. F., Bruckert, E., Fazio, S., Ference, B. A., Graham, I., Horton, J. D., Landmesser, U., Laufs, U., Masana, L., Pasterkamp, G., Raal, F. J., Ray, K. K., Schunkert, H., Taskinen, M. R., van de Sluis, B., Wiklund, O., Tokgozoglu, L., Catapano, A. L., and Ginsberg, H. N. (2020) Low-density lipoproteins cause atherosclerotic cardiovascular disease: pathophysiological, genetic, and therapeutic insights: a consensus statement from the European Atherosclerosis Society Consensus Panel. *Eur. Heart J.* **41**, 2313-2330
57. Lei, L., Xiong, Y., Chen, J., Yang, J. B., Wang, Y., Yang, X. Y., Chang, C. C., Song, B. L., Chang, T. Y., and Li, B. L. (2009) TNF-alpha stimulates the ACAT1 expression in differentiating monocytes to promote the CE-laden cell formation. *J. Lipid Res.* **50**, 1057-1067
58. An, S., Jang, Y. S., Park, J. S., Kwon, B. M., Paik, Y. K., and Jeong, T. S. (2008) Inhibition of acyl-coenzyme A:cholesterol acyltransferase stimulates cholesterol efflux from macrophages and stimulates farnesoid X receptor in hepatocytes. *Exp. Mol. Med.* **40**, 407-417
59. Satriano, J. A., Shuldiner, M., Hora, K., Xing, Y., Shan, Z., and Schlondorff, D. (1993) Oxygen radicals as second messengers for expression of the monocyte chemoattractant protein, JE/MCP-1, and the monocyte colony-stimulating factor, CSF-1, in response to tumor necrosis factor-alpha and immunoglobulin G. Evidence for involvement of reduced nicotinamide adenine dinucleotide phosphate (NADPH)-dependent oxidase. *J. Clin. Invest.* **92**, 1564-1571
60. Ding, A. H., Nathan, C. F., and Stuehr, D. J. (1988) Release of reactive nitrogen intermediates and reactive oxygen intermediates from mouse peritoneal macrophages. Comparison of activating cytokines and evidence for independent production. *J. Immunol.* **141**, 2407-2412
61. Trinh, M. N., Brown, M. S., Goldstein, J. L., Han, J., Vale, G., McDonald, J. G., Seemann, J., Mendell, J. T., and Lu, F. (2020) Last step in the path of LDL cholesterol from lysosome to plasma membrane to ER is governed by phosphatidylserine. *Proc. Natl. Acad. Sci. U. S. A.* **117**, 18521-18529
62. Hevonoja, T., Pentikainen, M. O., Hyvonen, M. T., Kovanen, P. T., and Ala-Korpela, M. (2000) Structure of low density lipoprotein (LDL) particles: basis for understanding molecular changes in modified LDL. *Biochim. Biophys. Acta* **1488**, 189-210

63. Mendivil, C. O., Rimm, E. B., Furtado, J., and Sacks, F. M. (2013) Apolipoprotein E in VLDL and LDL with apolipoprotein C-III is associated with a lower risk of coronary heart disease. *J Am Heart Assoc* **2**, e000130
64. Holtzman, D. M., Herz, J., and Bu, G. (2012) Apolipoprotein E and apolipoprotein E receptors: normal biology and roles in Alzheimer disease. *Cold Spring Harb. Perspect. Med.* **2**, a006312
65. Zhao, N., Liu, C. C., Qiao, W., and Bu, G. (2018) Apolipoprotein E, Receptors, and Modulation of Alzheimer's Disease. *Biol. Psychiatry* **83**, 347-357
66. Shan, L., Pang, L., Zhang, R., Murgolo, N. J., Lan, H., and Hedrick, J. A. (2008) PCSK9 binds to multiple receptors and can be functionally inhibited by an EGF-A peptide. *Biochem. Biophys. Res. Commun.* **375**, 69-73
67. Poirier, S., Mayer, G., Benjannet, S., Bergeron, E., Marcinkiewicz, J., Nassoury, N., Mayer, H., Nimpf, J., Prat, A., and Seidah, N. G. (2008) The proprotein convertase PCSK9 induces the degradation of low density lipoprotein receptor (LDLR) and its closest family members VLDLR and ApoER2. *J. Biol. Chem.* **283**, 2363-2372
68. Canuel, M., Sun, X., Asselin, M. C., Paramithiotis, E., Prat, A., and Seidah, N. G. (2013) Proprotein convertase subtilisin/kexin type 9 (PCSK9) can mediate degradation of the low density lipoprotein receptor-related protein 1 (LRP-1). *PLoS One* **8**, e64145
69. Ruiz, J., Kouiavskaia, D., Migliorini, M., Robinson, S., Saenko, E. L., Gorlatova, N., Li, D., Lawrence, D., Hyman, B. T., Weisgraber, K. H., and Strickland, D. K. (2005) The apoE isoform binding properties of the VLDL receptor reveal marked differences from LRP and the LDL receptor. *J. Lipid Res.* **46**, 1721-1731
70. Herz, J., Goldstein, J. L., Strickland, D. K., Ho, Y. K., and Brown, M. S. (1991) 39-kDa protein modulates binding of ligands to low density lipoprotein receptor-related protein/alpha 2-macroglobulin receptor. *J. Biol. Chem.* **266**, 21232-21238
71. Kraemer, F. B., Shen, W. J., Patel, S., Osuga, J., Ishibashi, S., and Azhar, S. (2007) The LDL receptor is not necessary for acute adrenal steroidogenesis in mouse adrenocortical cells. *Am. J. Physiol. Endocrinol. Metab.* **292**, E408-412
72. He, P., Gelissen, I. C., and Ammit, A. J. (2020) Regulation of ATP binding cassette transporter A1 (ABCA1) expression: cholesterol-dependent and - independent signaling pathways with relevance to inflammatory lung disease. *Respir. Res.* **21**, 250
73. Gerbod-Giannone, M. C., Li, Y., Holleboom, A., Han, S., Hsu, L. C., Tabas, I., and Tall, A. R. (2006) TNFalpha induces ABCA1 through NF-kappaB in macrophages and in phagocytes ingesting apoptotic cells. *Proc. Natl. Acad. Sci. U. S. A.* **103**, 3112-3117
74. Khovidhunkit, W., Moser, A. H., Shigenaga, J. K., Grunfeld, C., and Feingold, K. R. (2001) Regulation of scavenger receptor class B type I in hamster liver and Hep3B cells by endotoxin and cytokines. *J. Lipid Res.* **42**, 1636-1644
75. Simon, L., Campos, A., Leyton, L., and Quest, A. F. G. (2020) Caveolin-1 function at the plasma membrane and in intracellular compartments in cancer. *Cancer Metastasis Rev.* **39**, 435-453
76. Hubert, M., Larsson, E., Vegesna, N. V. G., Ahnlund, M., Johansson, A. I., Moodie, L. W., and Lundmark, R. (2020) Lipid accumulation controls the balance between surface connection and scission of caveolae. *Elife* **9**
77. Ogier, J. M., Nayagam, B. A., and Lockhart, P. J. (2020) ASK1 inhibition: a therapeutic strategy with multi-system benefits. *J. Mol. Med. (Berl.)* **98**, 335-348
78. Xia, X., Xu, Q., Liu, M., Chen, X., Liu, X., He, J., Hu, T., Yu, C., Huang, H., Liu, S., and Liu, N. (2020) Deubiquitination of CD36 by UCHL1 promotes foam cell formation. *Cell Death Dis.* **11**, 636
79. Ruuth, M., Nguyen, S. D., Vihervaara, T., Hilvo, M., Laajala, T. D., Kondadi, P. K., Gistera, A., Lahteenmaki, H., Kittila, T., Huusko, J., Uusitupa, M., Schwab, U., Savolainen, M. J., Sinisalo, J., Lokki, M. L., Nieminen, M. S., Jula, A., Perola, M., Yla-Herttula, S., Rudel, L., Oorni, A., Baumann,

M., Baruch, A., Laaksonen, R., Ketelhuth, D. F. J., Aittokallio, T., Jauhiainen, M., Kakela, R., Boren, J., Williams, K. J., Kovanen, P. T., and Oorni, K. (2018) Susceptibility of low-density lipoprotein particles to aggregate depends on particle lipidome, is modifiable, and associates with future cardiovascular deaths. *Eur. Heart J.* **39**, 2562-2573

80. Hurt, E., and Camejo, G. (1987) Effect of arterial proteoglycans on the interaction of LDL with human monocyte-derived macrophages. *Atherosclerosis* **67**, 115-126
81. Salisbury, B. G., Falcone, D. J., and Minick, C. R. (1985) Insoluble low-density lipoprotein-proteoglycan complexes enhance cholesteryl ester accumulation in macrophages. *Am. J. Pathol.* **120**, 6-11
82. Hurt, E., Bondjers, G., and Camejo, G. (1990) Interaction of LDL with human arterial proteoglycans stimulates its uptake by human monocyte-derived macrophages. *J. Lipid Res.* **31**, 443-454
83. Puig, N., Montolio, L., Camps-Renom, P., Navarra, L., Jimenez-Altayo, F., Jimenez-Xarrie, E., Sanchez-Quesada, J. L., and Benitez, S. (2020) Electronegative LDL Promotes Inflammation and Triglyceride Accumulation in Macrophages. *Cells* **9**
84. Malhotra, P., Gill, R. K., Saksena, S., and Alrefai, W. A. (2020) Disturbances in Cholesterol Homeostasis and Non-alcoholic Fatty Liver Diseases. *Front Med (Lausanne)* **7**, 467
85. Silverstein, R. L. (2021) PCSK9 (Proprotein Convertase Subtilisin/Kexin 9) Goes "DAMP". *Circulation* **143**, 62-64
86. Adorni, M. P., Zimetti, F., Lupo, M. G., Ruscica, M., and Ferri, N. (2020) Naturally Occurring PCSK9 Inhibitors. *Nutrients* **12**
87. Qi, Z., Hu, L., Zhang, J., Yang, W., Liu, X., Jia, D., Yao, Z., Chang, L., Pan, G., Zhong, H., Luo, X., Yao, K., Sun, A., Qian, J., Ding, Z., and Ge, J. (2021) PCSK9 (Proprotein Convertase Subtilisin/Kexin 9) Enhances Platelet Activation, Thrombosis, and Myocardial Infarct Expansion by Binding to Platelet CD36. *Circulation* **143**, 45-61
88. Sun, R., Peng, M., Xu, P., Huang, F., Xie, Y., Li, J., Hong, Y., Guo, H., Liu, Q., and Zhu, W. (2020) Low-density lipoprotein receptor (LDLR) regulates NLRP3-mediated neuronal pyroptosis following cerebral ischemia/reperfusion injury. *J. Neuroinflammation* **17**, 330
89. Zhao, S. P., and Dong, S. Z. (2008) Effect of tumor necrosis factor alpha on cholesterol efflux in adipocytes. *Clin. Chim. Acta* **389**, 67-71
90. Ma, K. L., Ruan, X. Z., Powis, S. H., Chen, Y., Moorhead, J. F., and Varghese, Z. (2008) Inflammatory stress exacerbates lipid accumulation in hepatic cells and fatty livers of apolipoprotein E knockout mice. *Hepatology* **48**, 770-781
91. Field, F. J., Watt, K., and Mathur, S. N. (2010) TNF-alpha decreases ABCA1 expression and attenuates HDL cholesterol efflux in the human intestinal cell line Caco-2. *J. Lipid Res.* **51**, 1407-1415
92. Wehmeier, K. R., Kurban, W., Chandrasekharan, C., Onstead-Haas, L., Mooradian, A. D., and Haas, M. J. (2016) Inhibition of ABCA1 Protein Expression and Cholesterol Efflux by TNF alpha in MLO-Y4 Osteocytes. *Calcif. Tissue Int.* **98**, 586-595
93. Zhao, S., Jiang, J., Jing, Y., Liu, W., Yang, X., Hou, X., Gao, L., and Wei, L. (2020) The concentration of tumor necrosis factor-alpha determines its protective or damaging effect on liver injury by regulating Yap activity. *Cell Death Dis.* **11**, 70
94. Gareb, B., Otten, A. T., Frijlink, H. W., Dijkstra, G., and Kosterink, J. G. W. (2020) Review: Local Tumor Necrosis Factor-alpha Inhibition in Inflammatory Bowel Disease. *Pharmaceutics* **12**
95. Del Valle, D. M., Kim-Schulze, S., Hsin-Hui, H., Beckmann, N. D., Nirenberg, S., Wang, B., Lavin, Y., Swartz, T., Madduri, D., Stock, A., Marron, T., Xie, H., Patel, M. K., van Oekelen, O., Rahman, A., Kovatch, P., Aberg, J., Schadt, E., Jagannath, S., Mazumdar, M., Charney, A., Firpo-Betancourt, A., Mendu, D. R., Jhang, J., Reich, D., Sigel, K., Cordon-Cardo, C., Feldmann, M., Parekh, S., Merad,

M., and Gnjatic, S. (2020) An inflammatory cytokine signature helps predict COVID-19 severity and death. *medRxiv*
96. Gerriets, V., Bansal, P., Goyal, A., and Khaddour, K. (2020) Tumor Necrosis Factor Inhibitors. in *StatPearls*, Treasure Island (FL). pp
97. Vasile, E., Simionescu, M., and Simionescu, N. (1983) Visualization of the binding, endocytosis, and transcytosis of low-density lipoprotein in the arterial endothelium in situ. *J. Cell Biol.* **96**, 1677-1689
98. Ghaffari, S., Jang, E., Naderinabi, F., Sanwal, R., Khosraviani, N., Wang, C., Steinberg, B. E., Goldenberg, N. M., Ikeda, J., and Lee, W. L. (2021) Endothelial HMGB1 Is a Critical Regulator of LDL Transcytosis via an SREBP2-SR-BI Axis. *Arterioscler. Thromb. Vasc. Biol.* **41**, 200-216
99. Molino, Y., David, M., Varini, K., Jabes, F., Gaudin, N., Fortoul, A., Bakloul, K., Masse, M., Bernard, A., Drobecq, L., Lecorche, P., Temsamani, J., Jacquot, G., and Khrestchatisky, M. (2017) Use of LDL receptor-targeting peptide vectors for in vitro and in vivo cargo transport across the blood-brain barrier. *FASEB J.* **31**, 1807-1827
100. Deane, R., Sagare, A., Hamm, K., Parisi, M., Lane, S., Finn, M. B., Holtzman, D. M., and Zlokovic, B. V. (2008) apoE isoform-specific disruption of amyloid beta peptide clearance from mouse brain. *J. Clin. Invest.* **118**, 4002-4013
101. Fisher, C., Beglova, N., and Blacklow, S. C. (2006) Structure of an LDLR-RAP complex reveals a general mode for ligand recognition by lipoprotein receptors. *Mol. Cell* **22**, 277-283
102. Havel, R., Eder, H., and Bragdon, J. (1955) The distribution and chemical composition of ultracentrifugally separated lipoproteins in human serum. *J Clin. Invest.* **34**, 1345-1353
103. Skipski, V. P., Barclay, M., Barclay, R. K., Fetzer, V. A., Good, J. J., and Archibald, F. M. (1967) Lipid composition of human serum lipoproteins. *Biochem. J.* **104**, 340-352
104. Kuchinskiene, Z., and Carlson, L. A. (1982) Composition, concentration, and size of low density lipoproteins and of subfractions of very low density lipoproteins from serum of normal men and women. *J. Lipid Res.* **23**, 762-769
105. Mahley, R. W., Innerarity, T. L., Rall, S. C., Jr., and Weisgraber, K. H. (1984) Plasma lipoproteins: apolipoprotein structure and function. *J. Lipid Res.* **25**, 1277-1294
106. Andreae, W. A. (1955) A sensitive method for the estimation of hydrogen peroxide in biological materials. *Nature* **175**, 859-860
107. Allain, C. C., Poon, L. S., Chan, C. S., Richmond, W., and Fu, P. C. (1974) Enzymatic determination of total serum cholesterol. *Clin. Chem.* **20**, 470-475
108. Bligh, E. G., and Dyer, W. J. (1959) A rapid method of total lipid extraction and purification. *Can. J. Biochem. Physiol.* **37**, 911-917
109. Kaluzny, M. A., Duncan, L. A., Merritt, M. V., and Epps, D. E. (1985) Rapid separation of lipid classes in high yield and purity using bonded phase columns. *J. Lipid Res.* **26**, 135-140
110. Pitas, R. E., Innerarity, T. L., Weinstein, J. N., and Mahley, R. W. (1981) Acetoacetylated lipoproteins used to distinguish fibroblasts from macrophages in vitro by fluorescence microscopy. *Arteriosclerosis* **1**, 177-185
111. Parthasarathy, S., Steinbrecher, U. P., Barnett, J., Witztum, J. L., and Steinberg, D. (1985) Essential role of phospholipase A2 activity in endothelial cell-induced modification of low density lipoprotein. *Proc. Natl. Acad. Sci. U. S. A.* **82**, 3000-3004
112. Burstein, M., Scholnick, H. R., and Morfin, R. (1970) Rapid method for the isolation of lipoproteins from human serum by precipitation with polyanions. *J. Lipid Res.* **11**, 583-595
113. McQuin, C., Goodman, A., Chernyshev, V., Kamentsky, L., Cimini, B. A., Karhohs, K. W., Doan, M., Ding, L., Rafelski, S. M., Thirstrup, D., Wiegraebe, W., Singh, S., Becker, T., Caicedo, J. C., and Carpenter, A. E. (2018) CellProfiler 3.0: Next-generation image processing for biology. *PLoS Biol.* **16**, e2005970

FOOTNOTES

Abbreviations: ACAT, acyl-CoA cholesterol acyltransferase; AP, apical; apo(X) , apolipoprotein X; BHT, butylated hydroxytoluene; BL, basolateral; CAB, cholesterol assay buffer, DB, dialysis buffer; DiL, 1,1′-Dioctadecyl-3,3,3′,3′-tetramethylindocarbocyanine perchlorate; DMSO, dimethyl sulfoxide; GAPDH, glyceraldehyde 3-phosphate dehydrogenase; FAF-BSA, fatty acid-free bovine serum albumin; FBS, fetal bovine serum; HDL3, high density lipoprotein 3; HRP, horse radish peroxidase; LDL, low density lipoprotein; LDLR, low density lipoprotein receptor; LRP, ldlr- related protein; mHBSS, modified Hanks' balanced salt solution; PBS, phosphate buffered saline; PCSK9, proprotein convertase subtilisin/kexin type 9; pHAECs, primary human aortic endothelial cells; RAP, receptor associated protein; SDS, sodium dodecyl sulfate; TMTU, tetramethylthiourea; TNFα, tumor necrosis factor alpha; VBM, vascular basal medium; VEGF, vascular endothelial growth factor kit;

FIGURE LEGENDS

Figure 1. TNFα enhances cholesterol accumulation and LDL binding to pHAECs. A-B, pHAECs were treated with the indicted concentration of human LDL without (Ctrl) or with 100 ng/ml TNFα for 24 hours. Unesterified cholesterol and cholesteryl esters were determined as described under Experimental Procedures. n= 5. **C**, Cells were pre-treated with 0 or 5 ng/ml TNFα in serum medium as described under Experimental Procedures. After incubation at 37 °C, the amount of ^{125}I-LDL released to serum-free medium at 4 ºC without (0) or with 20 folds unlabeled LDL competitor (+) was determined as the surface ^{125}I-LDL. **D**, The experiment was performed as in E, and the amount of radioactivity associated with the cell was determined. C-D, n =3. *,**,***, p< 0.05, 0.01, 0.001, relative to the corresponding Ctrl.

Figure 2. ACAT inhibitor does not prevent TNFα-induced LDL cholesterol accumulation. Cells in serum-free medium were treated with 0 or 100 ng/ml TNFα in the presence of 0.1% DMSO (DMSO) or 10 µg/ml ACAT inhibitor (Sandoz 58-035) and 100 µg/ml LDL for 24 hrs. After washing with heparin as described under Experimental Procedures, the cellular cholesterol content was determined. n = 3. *,**,***, p< 0.05, 0.01, 0.001, relative to corresponding Ctrl or as indicated with bars.

Figure 3. LDL oxidation is not required for TNFα-induced LDL accumulation. A-B, Cells were treated with 0 (Ctrl) or 100 ng/ml TNFα (TNFα) for 24 hrs in serum medium. The media were replaced with serum-free media in the continued presence of TNFα for 2 hrs to remove surface lipoproteins. Finally, 5 µg/ml Dil-LDL in serum-free medium (Dil-LDL) ± 40 times LDL (+40X LDL) or oxLDL (+40X oxLDL) was added, followed by 3 hour incubation. The images are 20X magnifications. n = 3. ***, p< 0.001 vs. Ctrl. $, ###, p<0.05, 0.001, relative to Dil-LDL alone.

Figure 4. TNFα induces massive Dil over [^{3}H]CE lipid accumulation from LDL.
pHAECs in serum medium were pre-treated with the indicated concentration of human TNFα for 24 hrs. Subsequently, the cells were treated in the continued presence of the previous TNFα concentration and 50 µg/ml [^{3}H]CE-LDL (**A**) or 5 µg/ml Dil-LDL (**B**) without serum for 24 hrs. A, n =4, B, n =3. The cells were treated without (Ctrl), (**C)**, or with 100 ng/ml TNFα (**D**), as above, in the presence of increasing concentration of Dil-LDL. n = 5. *,**,*** ,p< 0.05, 0.01, 0.001, relative to 0 ng/ml TNFα or 1 µg/ml Dil-

LDL. #, ##, p< 0.05, 0.01, vs. previous TNFα dose. $$, $$$, p<0.01, 0.001, relative to the corresponding Dil-LDL concentration under Ctrl condition.

Figure 5. Lysosomal inhibitor enhances TNFα-induced LDL lipid accumulation. The cells were pre-treated with 0 or 100 ng/ml TNFα (+) for 24 hrs in the presence of serum. Subsequently, in the continued presence of TNFα, the cells were treated with 0.5 µg/ml Dil-LDL, plus 50 or 200 µg/ml [^{3}H]CE-LDL, and containing 0 or 50 µM chloroquine diphosphate (Cl-quine), +, a lysosomal blocker, without serum. After 24 hrs, the intracellular fluorescence (**A-B**) or radioactivity (**C**) was determined. The separation of #cells in A is an artificact of preparation prior to lysing the cells for radioactivity. The circumferential accumulation of the Dil-LDL in the presence of chloroquine is apparent (A). The images are 20X magnifications. n = 2.

Figure 6. ApoE is not required for TNFα-induced Dil-LDL accumulation. A, Dil-HDL3 or Dil-LDL was depleted of apoE (-), or apoE was retained (+) as described under Materials and Methods. The presence of apoB and apoE were determined by immunoblotting 0.5 and 1 µg/ml Dil-HDL3 and Dil-LDL, respectively. **B**, pHAECs were treated ± 100 ng/ml TNFα in serum medium for 24 hrs. Following 2 hr incubation in serum free medium, in the continued presence of TNFα, the cells were incubated with 2.5 µg/ml Dil-LDL without (-) or with apoE (+) for 3 hrs.

Figure 7. TNFα-induced Dil-LDL accumulation is blocked by specific LDLR antibody. A, pHAECs in serum medium were pre-treated with 0 (Ctrl) or 100 ng/ml TNFα for 24 hrs. Afterwards, the cells were cultured in the presence of vehicle, 12.5 µg/ml human PCSK9 (ApoER, LDLR, LRP, and VLDLR inhibitors), or 21 µg/ml human RAP (ApoER2, LRP, and VLDLR inhibitors) in serum-free medium for 1 hr. Lastly, 8 µg/ml Dil-LDL was added, followed by 4 hr incubation. n = 3. **B**, Mouse immorto hepatocytes were incubated in serum-free RPMI 1640 medium containing vehicle or RAP as above for 1 hr. Lastly, the hepatocytes were incubated for 2 hrs with Dil-LDL. n = 1. ###, ***, p< 0.001 vs Ctrl vehicle and TNFα vehicle, respectively. **C**, Cells were cultured in serum medium ± 100 ng/ml TNFα, followed by 3 hr incubation in serum-free medium in the continued presence of TNFα (+) without antibody (None), 18 µg/ml control IgG (Ctrl Ig) or LDLR antibody (LDLR), then immunoblotted for LDLR and GAPDH. n = 3. **D**, pHAECs were cultured in serum-free medium for 2 hrs, followed by incubation with 5 µg/ml Dil-HDL3 with (+) 134X unlabeled HDL3, LDL, 20 µg/ml control IgG (Ctrl IgG) or LDLR antibody (LDLR Ab), as indicated. n = 6. ***, p< 0.001 vs Dil-HDL3. **E**, Cells were cultured in serum medium with 0 or 100 ng/ml TNFα (+), followed by 2 hr incubation in serum-free medium in the continued presence of TNFα. Subsequently, 5 µg/ml Dil-LDL in the presence of 20 µg/ml control IgG (Ctrl IgG) or LDLR antibody (LDLR Ab) was added. Note that the values for LDLR Ab are very low compared to others. n = 8. ###, ***, p< 0.001 vs. corresponding 0 µg/ml TNFα and Ctrl IgG, respectively.

Figure 8. TNFα upregulates cell surface LDLR protein. A-F, Confluent pHAECs in serum medium were pre-treated with 0 or 100 ng/ml TNFα (+) for 24 hrs in serum medium. The cells were then treated and lysed for total (Total Lysates) and biotinylated cell surface (Cell Surface) proteins, as explained under Experimental Procedures. ABCA1 bands (A,B) at ~ 220 and 110 kD are indicated. n = 3. *,**,*** ,p< 0.05, 0.01, 0.001, vs corresponding Ctrl.

Figure 9. TNFα promotes rapid association of LDLR with it antibody. pHAECs in serum medium were pre-treated with 0 (Ctrl) or 100 ng/ml TNFα (TNFα) for 24 hrs. Subsequently, in the continued presence of TNFα, the media were replaced with 5 µg/ml control normal goat IgG or LDLR antibody

(LDLR Ab) for 0, 5, 30, or 120 minutes at 37 °C. The surface-accessible LDLR was then determined as detailed under Experimental Procedures. **A**, 20X objective magnification of LDLR detected after 30 minutes. **B**, 40X confocal detection of LDLR in TNFα-treated pHAECs at 0 and 5 minutes. The arrows show the membrane distribution of the LDLR in focus, while the arrowhead shows internalized LDLR. **C**, Surface-accessible LDLR as a function of time under control condition. **D**, As C, in the presence of TNFα. nN = 4. **, p< 0.01 relative to control at the same time.

Figure 10. Anti-oxidant suppresses TNFα-induced Dil-LDL accumulation. A, pHAECs were pre-treated with 0.05% DMSO (Vehicle) or TNFα-cascade inhihitors, as indicated: NF-kBi (25 µM). Two different forms were tested. ASK1i (5 µM), p38i (1 µM), JNKi (5 µM), or pan-caspase inhibitor, Caspasei (5 µM) for 30 minutes in serum-free medium. Subsequently, serum-free 3 µg/ml Dil-LDL, with 100 ng/ml TNFα, as indicated, was added, followed by 24 hr incubation. n = 3. **B**, Cells were treated with 1% DMSO vehicle with 100 ng/ml TNFα as indicated, in the presence of 0, 1, 5, or 20 mM TMTU and 3 µg/ml Dil-LDL. Subsequently, the cells were cultured for 24 hrs. n = 4. ***, ###, p< 0.001 vs. 0 µg/ml TNFα and 0 mM TMTU in the presence of TNFα, respectively.

Figure 11. TNFα does not affect AP to BL release of degraded LDL protein. A, Diagram of the experimental setup in B-C, in which pHAECs were grown to confluence on 3 µm polycarbonate filters, with ^{125}I-LDL in the AP medium. **B**, pHAECs in serum medium were pre-treated with 0 (Ctrl) or 5 ng/ml TNFα on the BL side for 48 hrs. Then 10 µg/ml ^{125}I-LDL without serum was added to the AP side (No Competitor) or with 30 folds unlabeled LDL (+)30X LDL, in the continued presence of TNFα. After 3 hours, the BL media were collected, and non-intact ^{125}I-LDL was measured as described under Experimental Procedures. **C**, The experiment was performed as in B, followed by detection of intact BL ^{125}I-LDL. n =3.*,**, p< 0.05, 0.01, respectively,

Figure 12. TNFα does not affect AP to BL LDL lipid release. A-D, pHAECs were pre-treated as in Figure 11 with 0, 10, or 100 ng/ml TNFα for 24 hrs in serum. Subsequently, 20 µg/ml control normal goat IgG (Goat IgG) or LDLR antibody (LDLR Ab) was added to the AP medium without serum for 2 hrs. Finally, 1.6 mg/ml double labeled Dil,[^{3}H]CE-LDL was added to the AP medium for 3 hrs. After heparin wash, the intracellular fluorescence (**A-B**), ^{3}H radioactivity (**C**), or medium BL ^{3}H (**D**) was determined. **E**, The cells were treated for 3 or 24 hrs with 0 (Ctrl) or 100 ng/ml TNFα without serum in the presence of apical Dil-LDL, and the BL fluorescence was determined. n = 3.

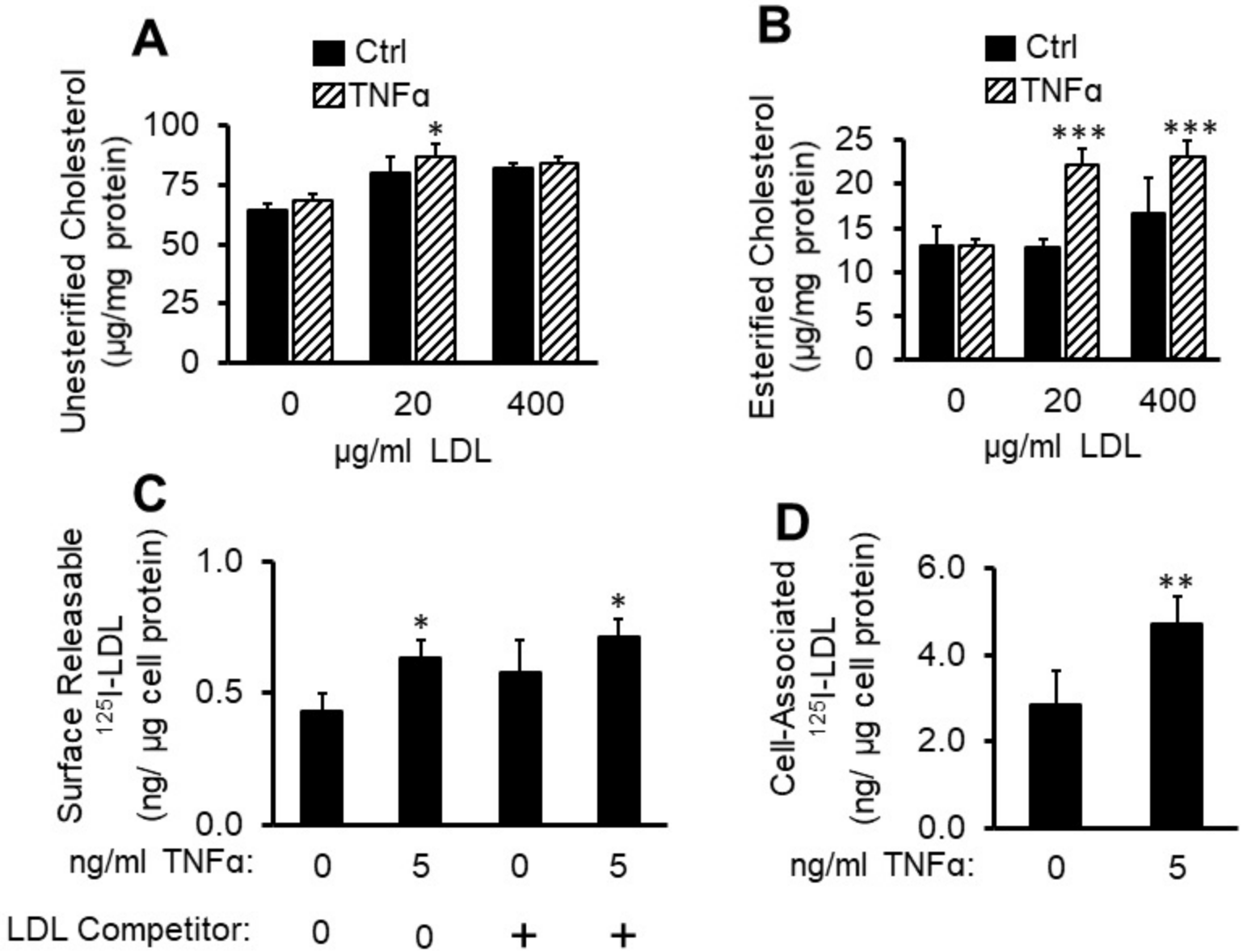
A
Ctrl
TNFα
Unesterified Cholesterol (µg/mg protein)
100
75
50
25
0
*
0
20
400
µg/ml LDL
B
Ctrl
TNFα
Esterified Cholesterol (µg/mg protein)
25
20
15
10
5
0
***
***
0
20
400
µg/ml LDL
C
Surface Releasable 125I-LDL (ng/ µg cell protein)
1.0
0.5
0.0
*
*
ng/ml TNFα: 0 5 0 5
LDL Competitor: 0 0 + +
D
Cell-Associated 125I-LDL (ng/ µg cell protein)
6.0
4.0
2.0
0.0
**
ng/ml TNFα: 0 5

Figure 1

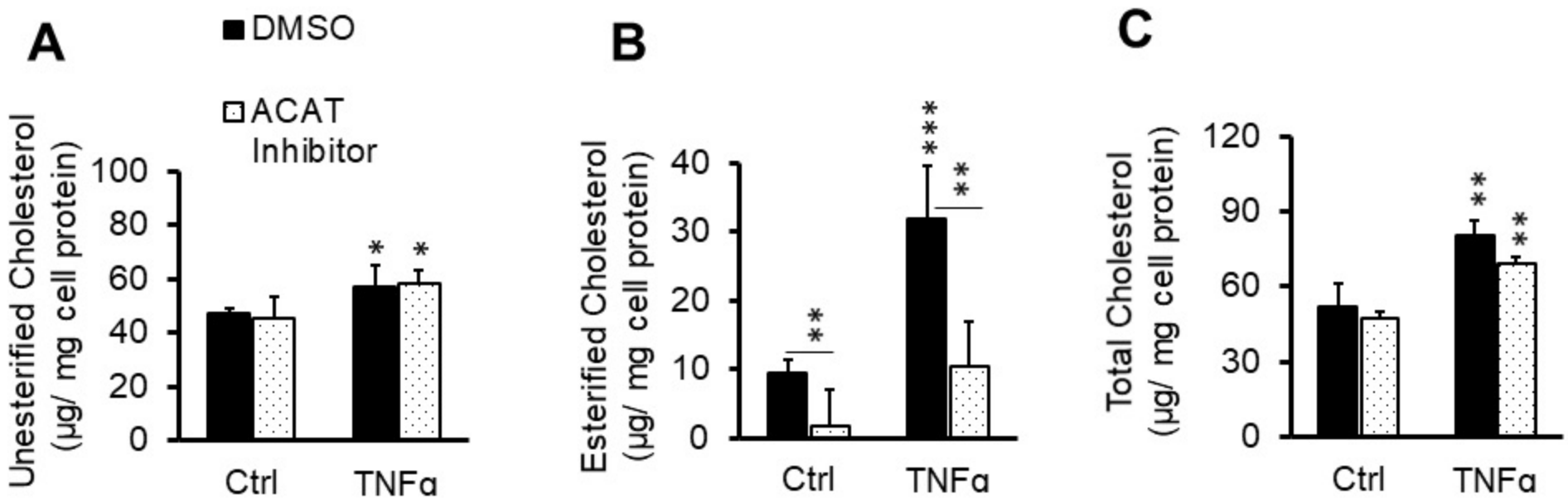
A
DMSO
ACAT Inhibitor
Unesterified Cholesterol (µg/ mg cell protein)
100
80
60
40
20
0
Ctrl
TNFα
B
Esterified Cholesterol (µg/ mg cell protein)
40
30
20
10
0
Ctrl
TNFα
C
Total Cholesterol (µg/ mg cell protein)
120
90
60
30
0
Ctrl
TNFα

Figure 2

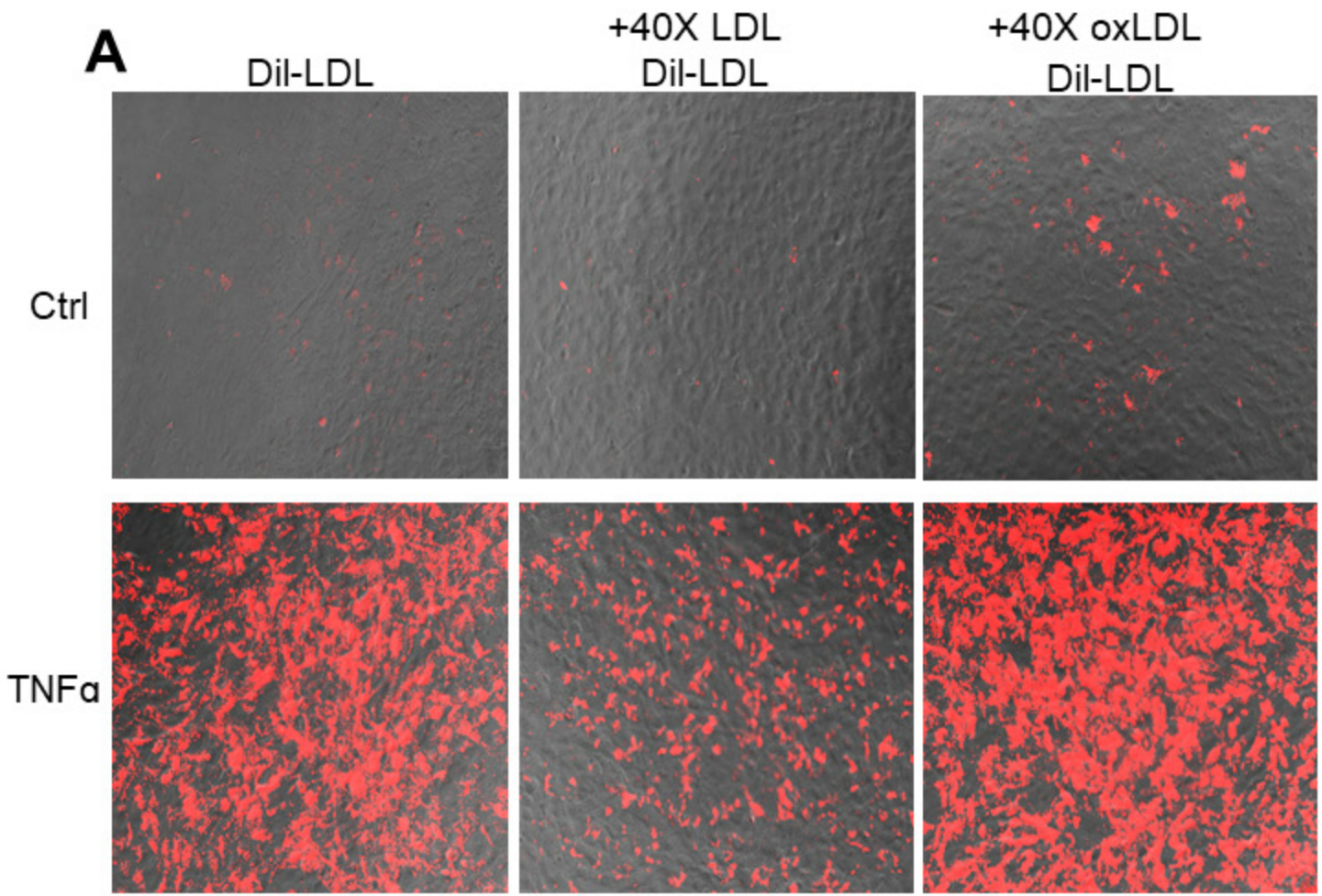
A
Dil-LDL
+40X LDL
Dil-LDL
+40X oxLDL
Dil-LDL
Ctrl
TNFα

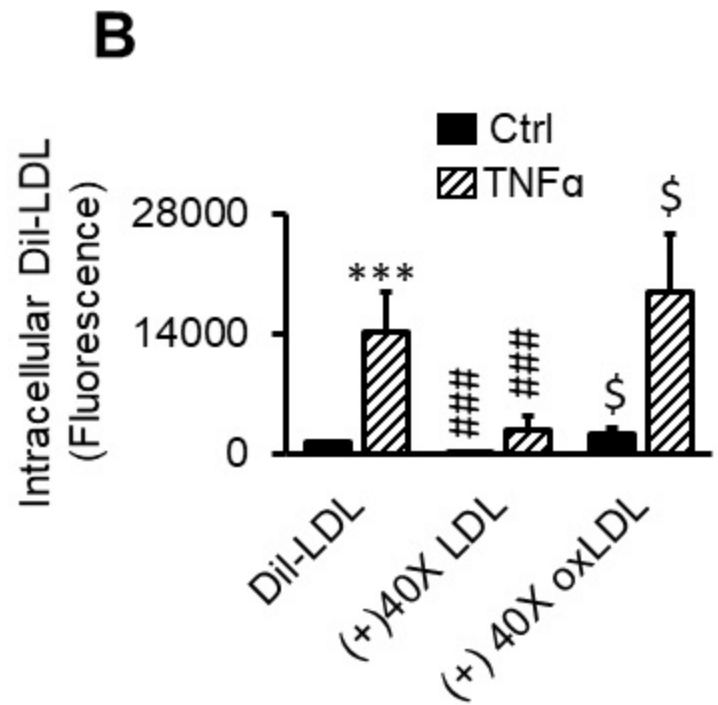
B
Ctrl
TNFα
Intracellular Dil-LDL
(Fluorescence)
28000
14000
0
***
###
###
$
$
Dil-LDL
(+)40X LDL
(+) 40X oxLDL

Figure 3

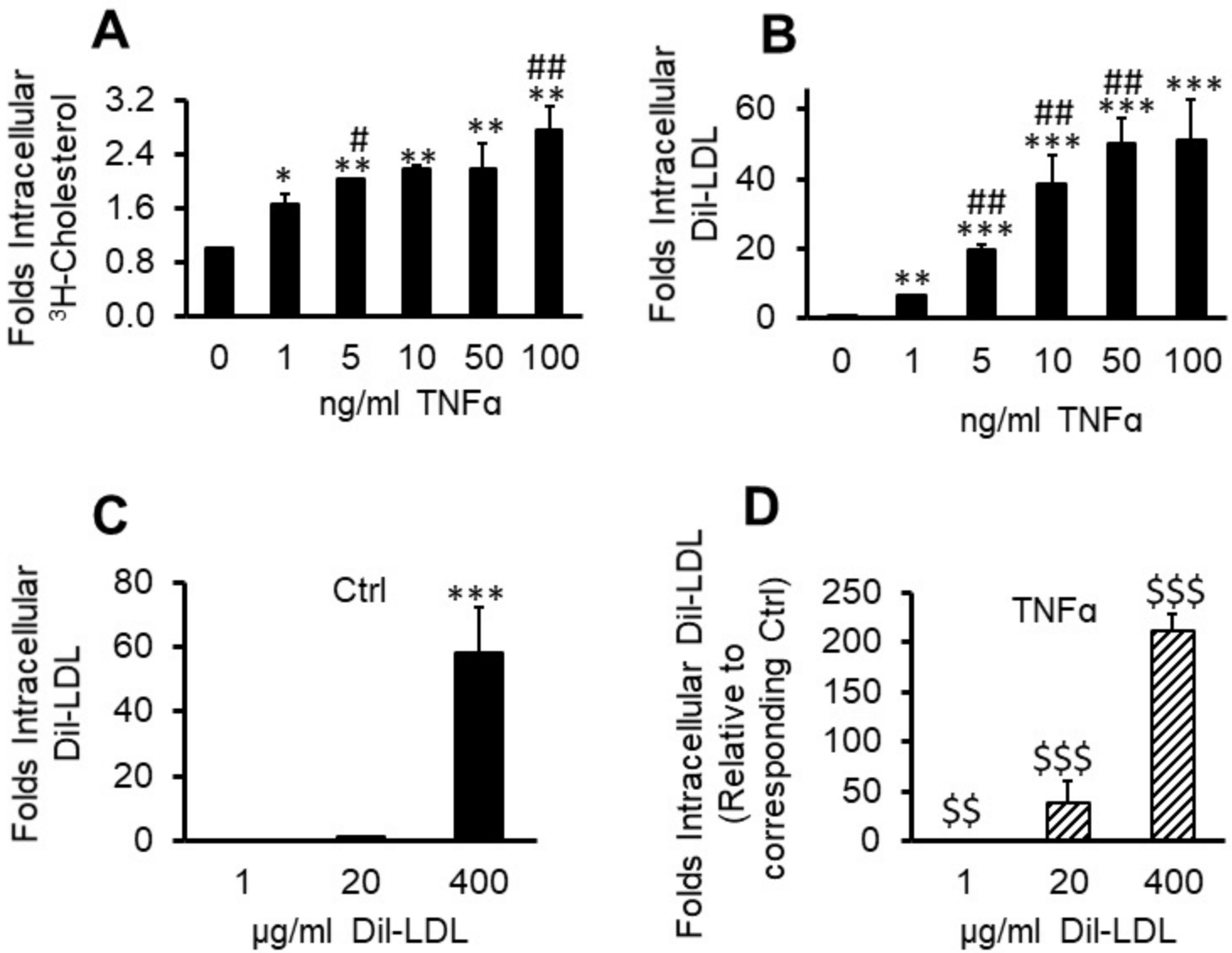
A
Folds Intracellular
3H-Cholesterol
3.2
2.4
1.6
0.8
0.0
0
1
5
10
50
100
ng/ml TNFα
B
Folds Intracellular
Dil-LDL
60
40
20
0
ng/ml TNFα
C
Folds Intracellular
Dil-LDL
80
60
40
20
0
Ctrl
1
20
400
µg/ml Dil-LDL
D
Folds Intracellular Dil-LDL
(Relative to
corresponding Ctrl)
250
200
150
100
50
0
TNFα
$$
$$$
1
20
400
µg/ml Dil-LDL

Figure 4

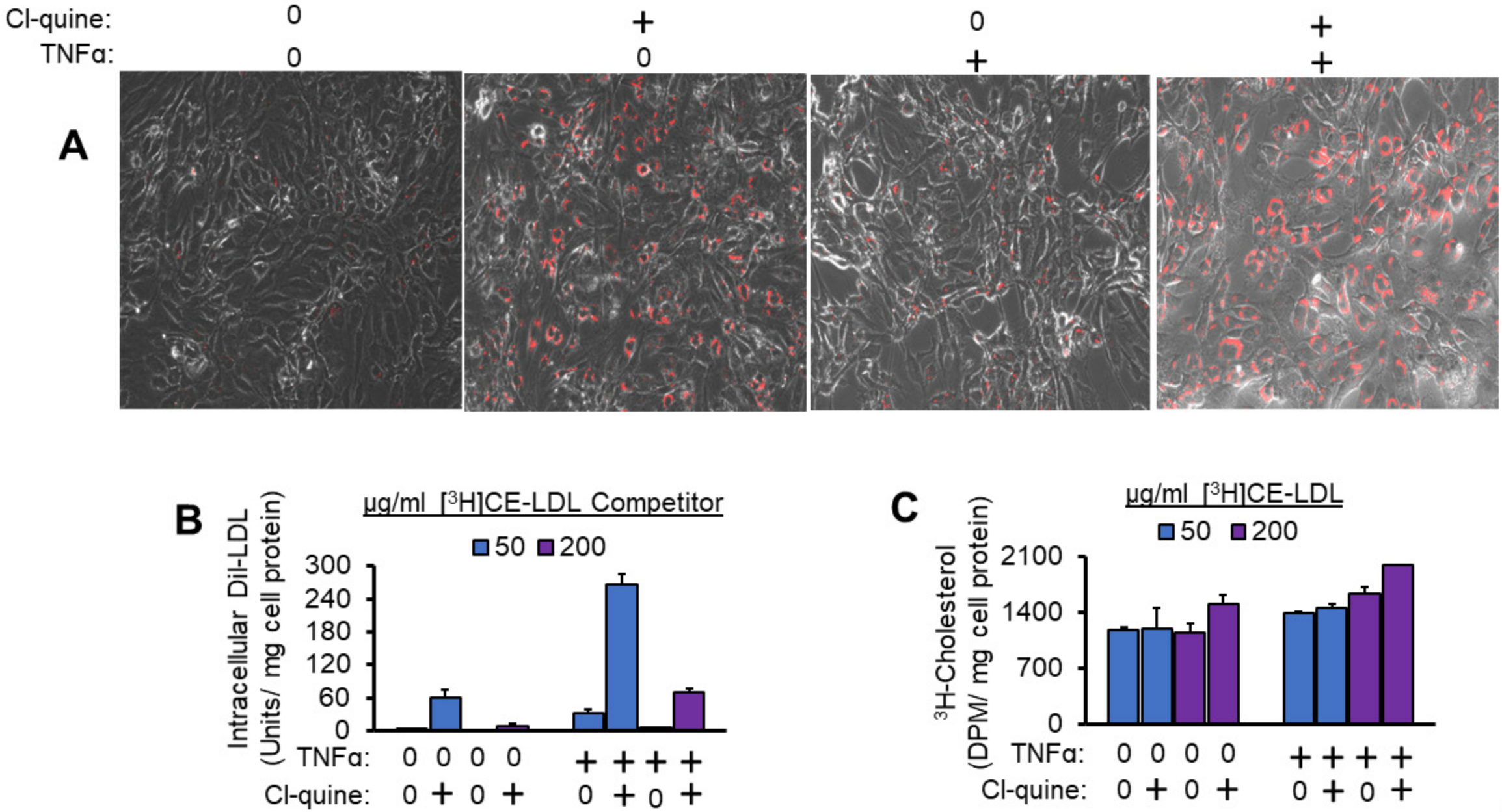
Cl-quine: 0 + 0 +
TNFα: 0 0 + +
A
B
Intracellular Dil-LDL (Units/ mg cell protein)
µg/ml [3H]CE-LDL Competitor
50 200
300
240
180
120
60
0
TNFα: 0 0 0 0 + + + +
Cl-quine: 0 + 0 + 0 + 0 +
C
3H-Cholesterol (DPM/ mg cell protein)
µg/ml [3H]CE-LDL
50 200
2100
1400
700
0
TNFα: 0 0 0 0 + + + +
Cl-quine: 0 + 0 + 0 + 0 +

Figure 5

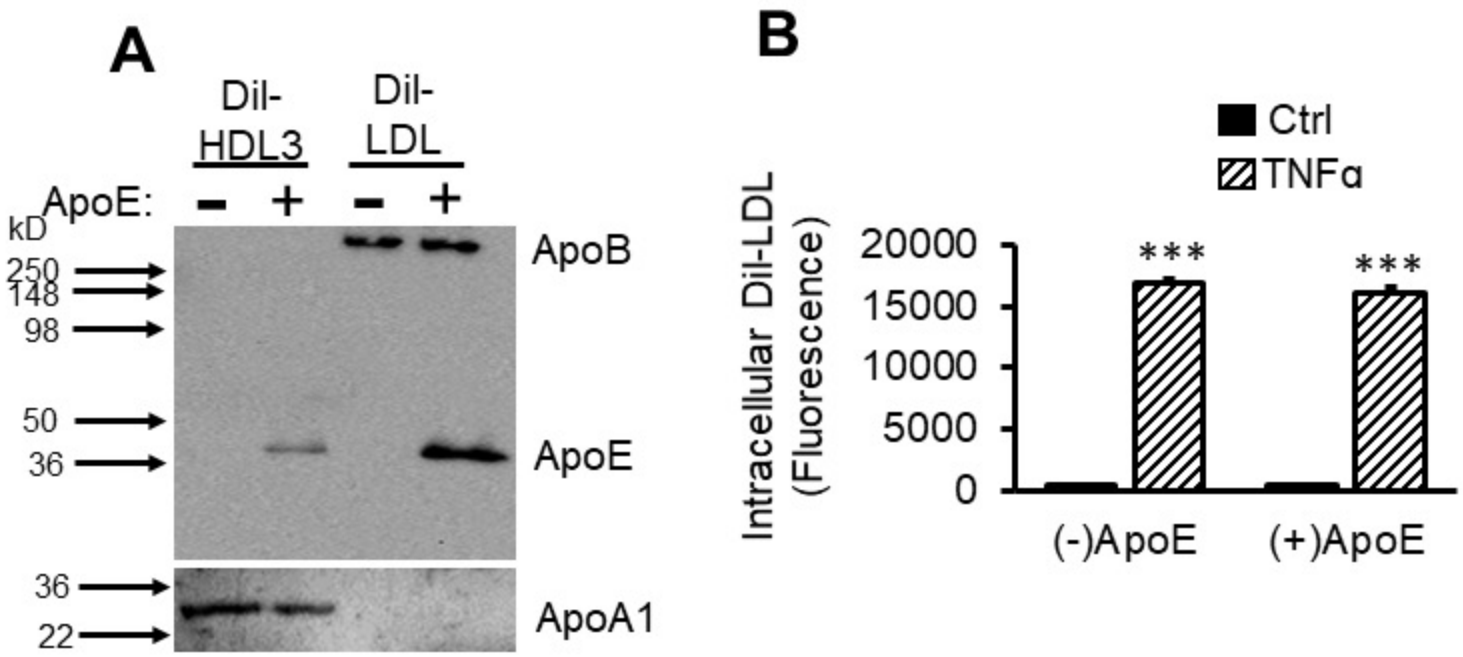
A
Dil-HDL3
Dil-LDL
ApoE:
-
+
-
+
kD
250
148
98
50
36
36
22
ApoB
ApoE
ApoA1
B
Ctrl
TNFα
Intracellular Dil-LDL (Fluorescence)
20000
15000
10000
5000
0
***
***
(-)ApoE
(+)ApoE

Figure 6

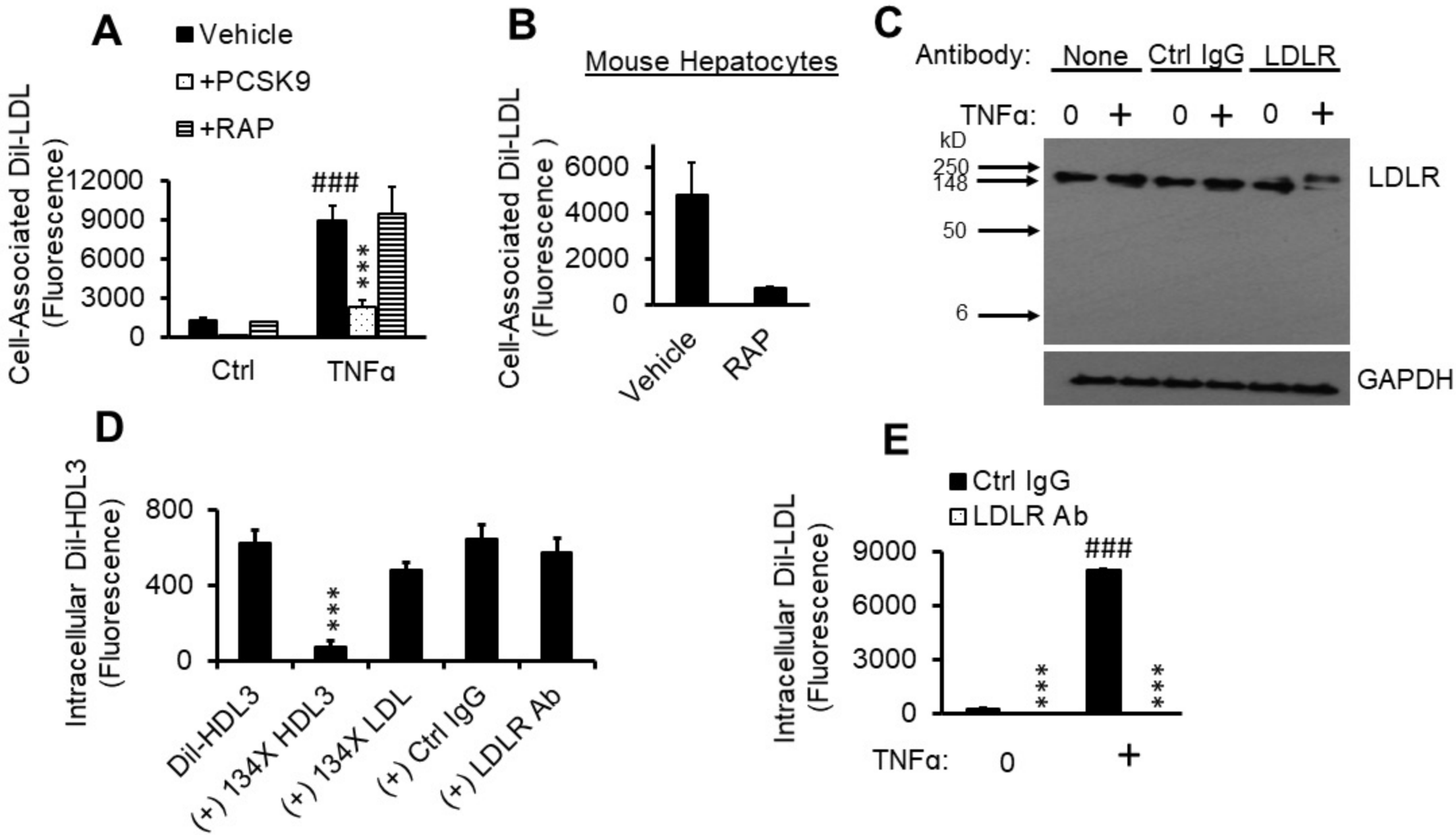
A
Vehicle
+PCSK9
+RAP
Cell-Associated Dil-LDL (Fluorescence)
12000
9000
6000
3000
0
###
***
Ctrl
TNFα
B
Mouse Hepatocytes
Cell-Associated Dil-LDL (Fluorescence)
6000
4000
2000
0
Vehicle
RAP
C
Antibody: None Ctrl IgG LDLR
TNFα: 0 + 0 + 0 +
kD
250
148
50
6
LDLR
GAPDH
D
Intracellular Dil-HDL3 (Fluorescence)
800
400
0
***
Dil-HDL3
(+) 134X HDL3
(+) 134X LDL
(+) Ctrl IgG
(+) LDLR Ab
E
Ctrl IgG
LDLR Ab
Intracellular Dil-LDL (Fluorescence)
9000
6000
3000
0
###
***
***
TNFα: 0 +

Figure 7

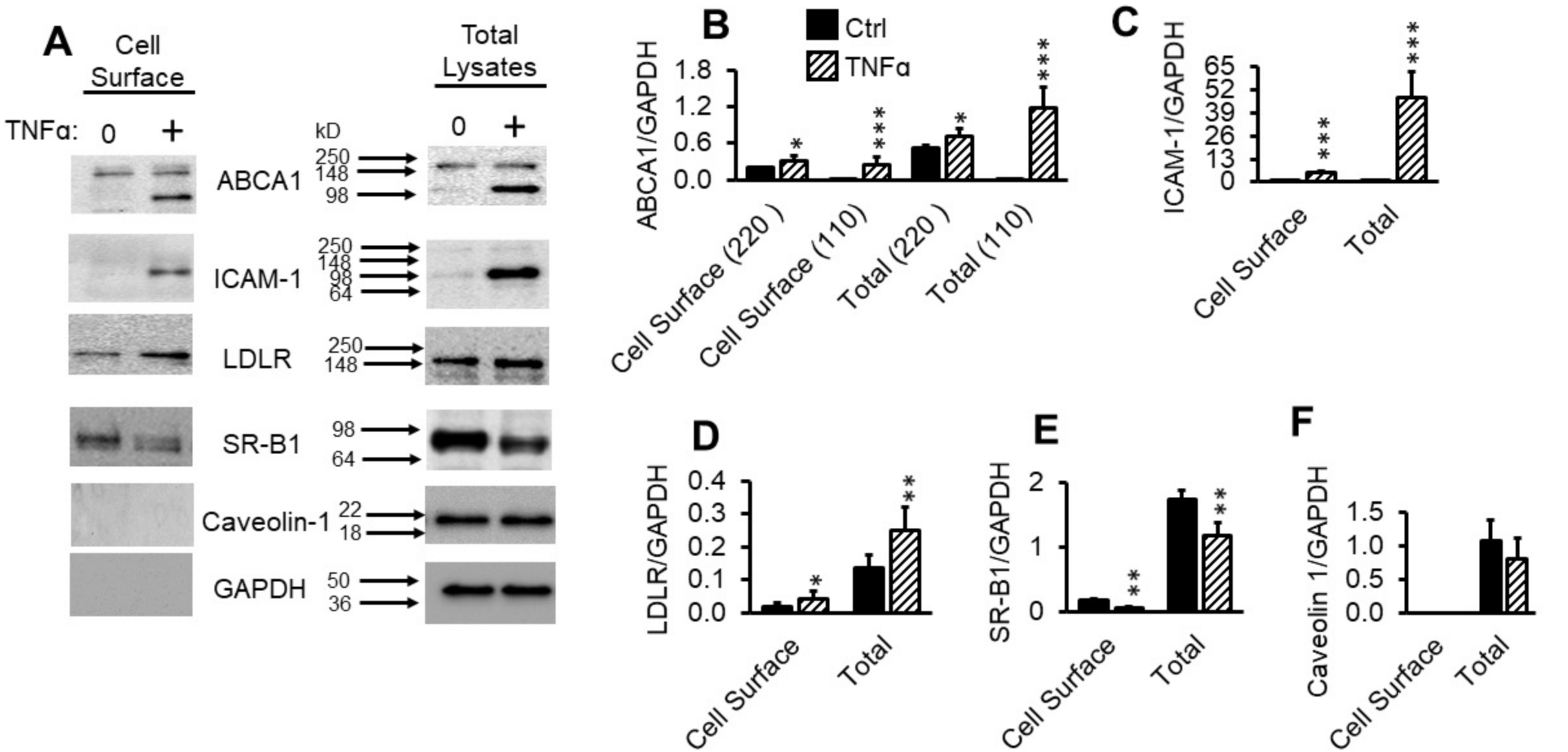
A
Cell Surface
Total Lysates
TNFα: 0 +
kD
0 +
ABCA1
250
148
98
ICAM-1
250
148
98
64
LDLR
250
148
SR-B1
98
64
Caveolin-1
22
18
GAPDH
50
36
B
Ctrl
TNFα
ABCA1/GAPDH
1.8
1.2
0.6
0.0
Cell Surface (220)
Cell Surface (110)
Total (220)
Total (110)
C
ICAM-1/GAPDH
65
52
39
26
13
0
Cell Surface
Total
D
LDLR/GAPDH
0.4
0.3
0.2
0.1
0.0
Cell Surface
Total
E
SR-B1/GAPDH
2
1
0
Cell Surface
Total
F
Caveolin 1/GAPDH
1.5
1.0
0.5
0.0
Cell Surface
Total

Figure 8

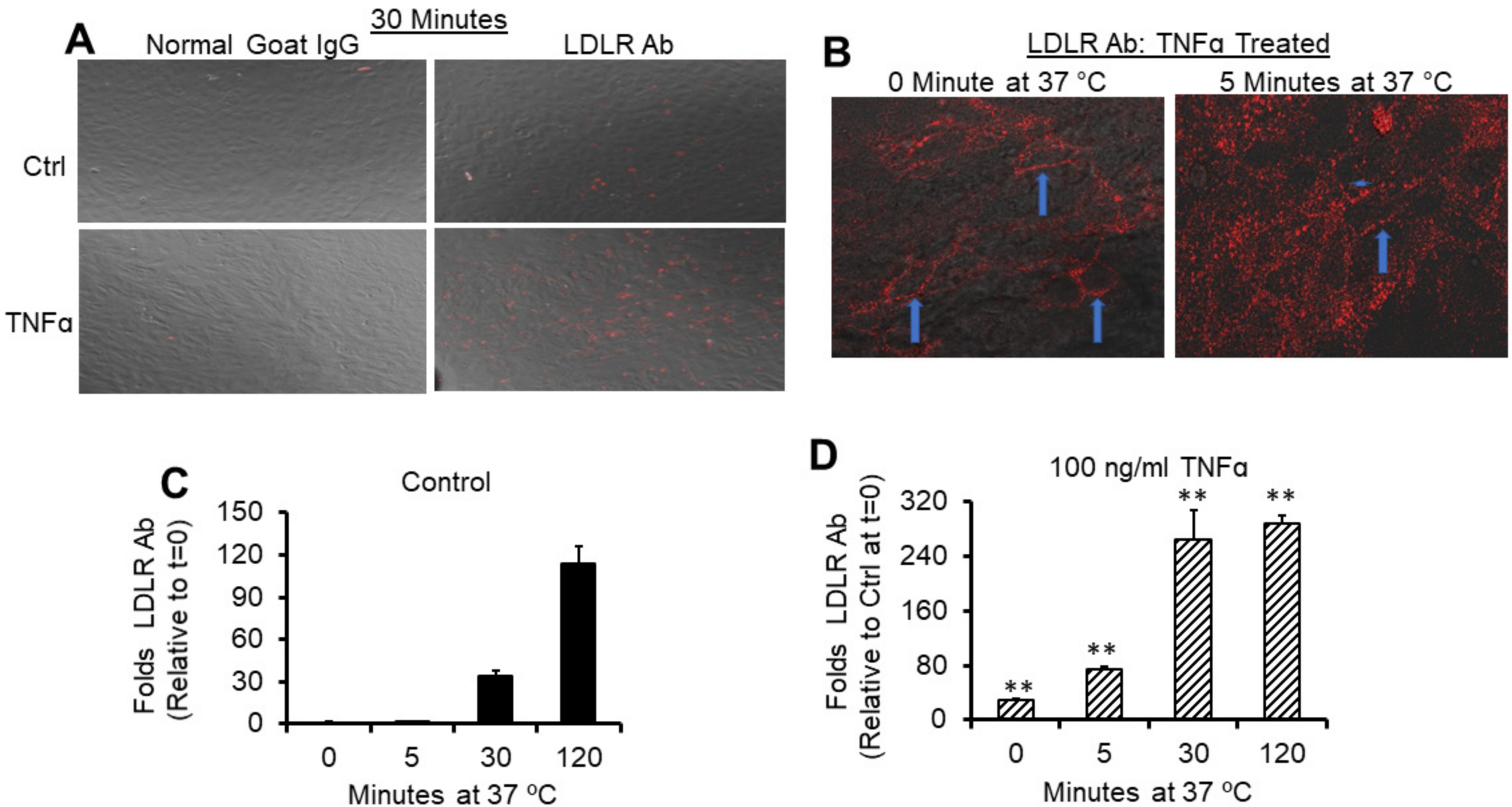
A
30 Minutes
Normal Goat IgG
LDLR Ab
Ctrl
TNFα
B
LDLR Ab: TNFα Treated
0 Minute at 37 °C
5 Minutes at 37 °C
C
Control
Folds LDLR Ab (Relative to t=0)
150
120
90
60
30
0
0
5
30
120
Minutes at 37 °C
D
100 ng/ml TNFα
Folds LDLR Ab (Relative to Ctrl at t=0)
320
240
160
80
0
**
**
**
**
0
5
30
120
Minutes at 37 °C

Figure 9

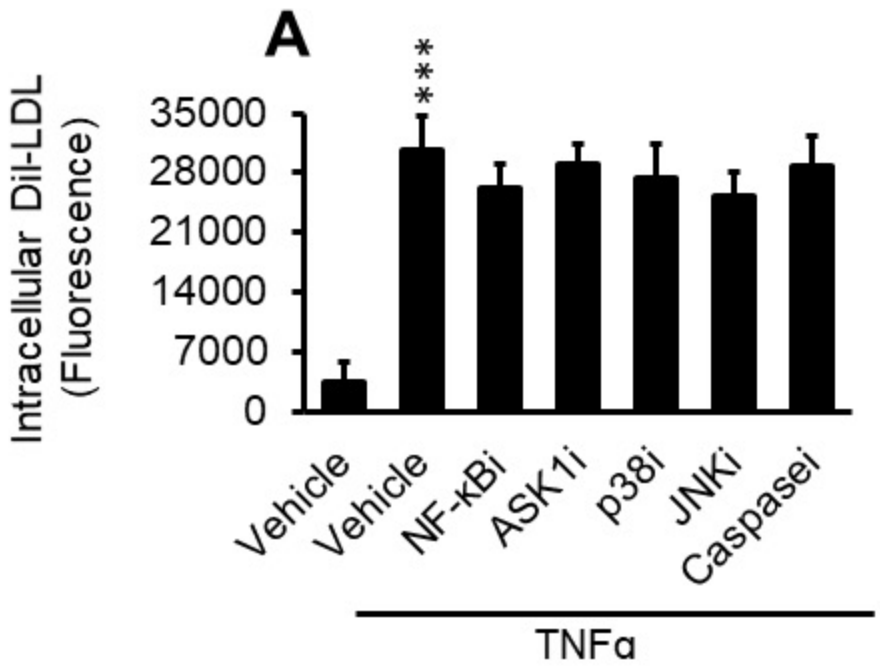
A
Intracellular Dil-LDL (Fluorescence)
35000
28000
21000
14000
7000
0
***
Vehicle
Vehicle
NF-κBi
ASK1i
p38i
JNKi
Caspasei
TNFα

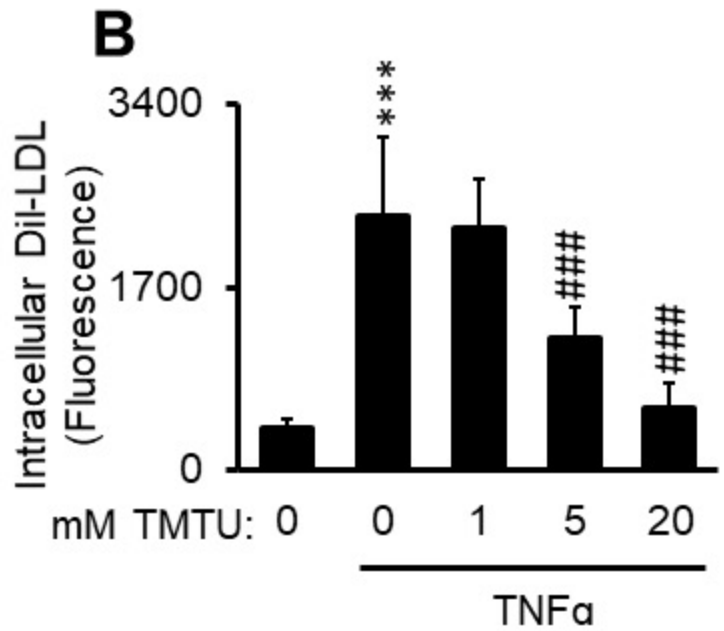
B
Intracellular Dil-LDL (Fluorescence)
3400
1700
0
***
###
###
mM TMTU: 0 0 1 5 20
TNFα

Figure 10

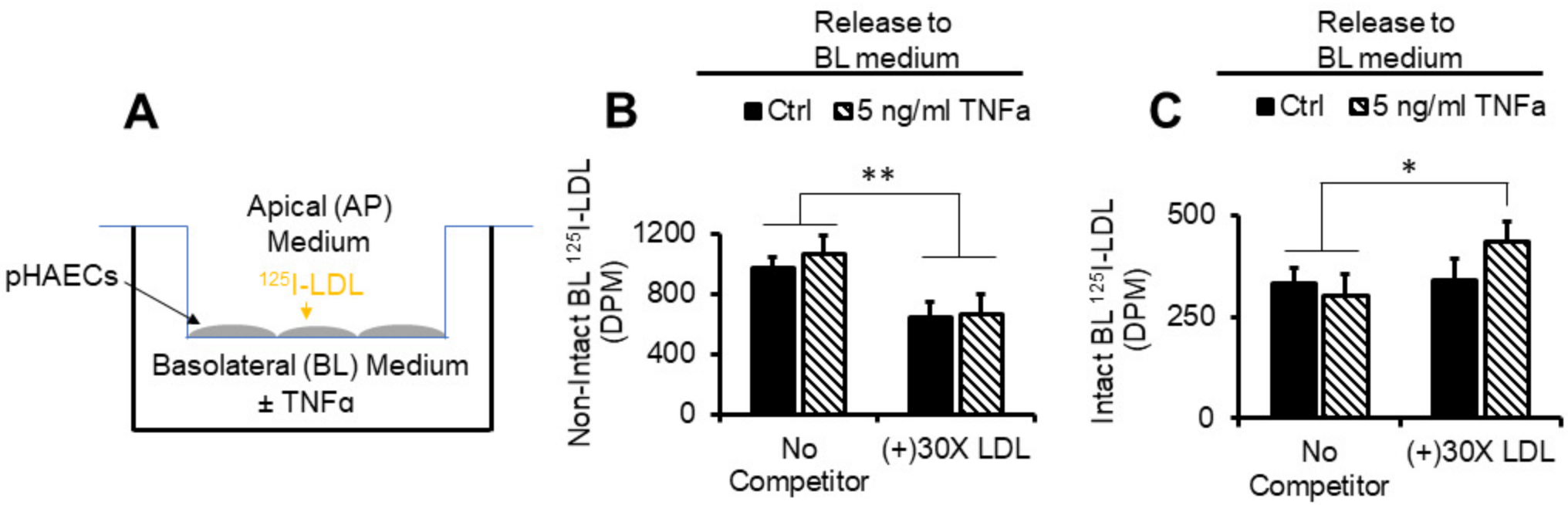
A
Apical (AP)
Medium
pHAECs
125I-LDL
Basolateral (BL) Medium
± TNFα
B
Release to
BL medium
Ctrl
5 ng/ml TNFa
**
Non-Intact BL 125I-LDL
(DPM)
1200
800
400
0
No
Competitor
(+)30X LDL
C
Release to
BL medium
Ctrl
5 ng/ml TNFa
*
Intact BL 125I-LDL
(DPM)
500
250
0
No
Competitor
(+)30X LDL

Figure 11

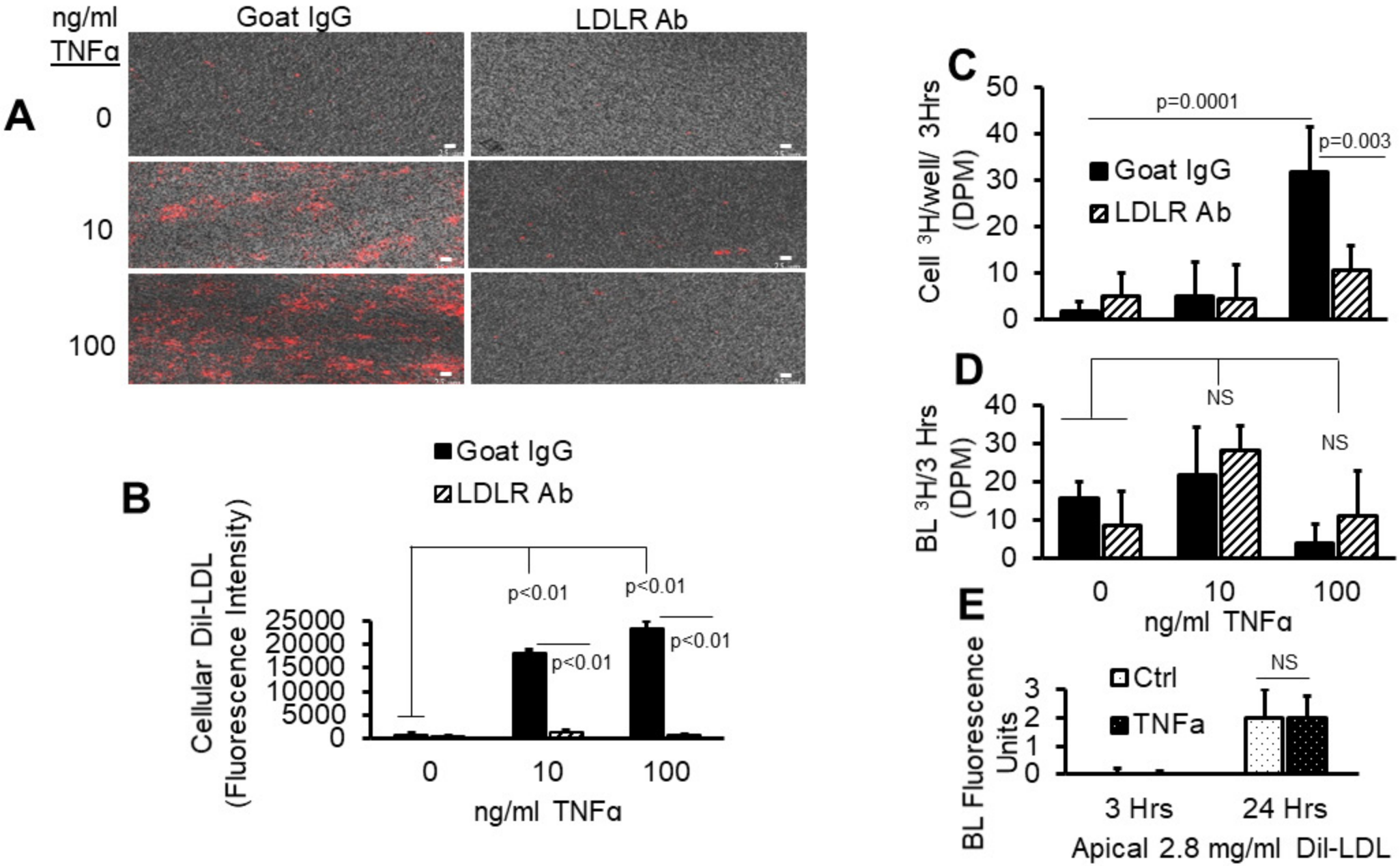
A
ng/ml TNFα
Goat IgG
LDLR Ab
0
10
100
B
Goat IgG
LDLR Ab
Cellular Dil-LDL (Fluorescence Intensity)
25000
20000
15000
10000
5000
0
p<0.01
p<0.01
p<0.01
p<0.01
0
10
100
ng/ml TNFα
C
Cell ³H/well/ 3Hrs (DPM)
50
40
30
20
10
0
p=0.0001
p=0.003
Goat IgG
LDLR Ab
D
BL ³H/3 Hrs (DPM)
40
30
20
10
0
NS
NS
0
10
100
ng/ml TNFα
E
BL Fluorescence Units
3
2
1
0
Ctrl
TNFa
NS
3 Hrs
24 Hrs
Apical 2.8 mg/ml Dil-LDL

Figure 12